Cells

The osteoblastic cell line MC3T3-E1, which was established from normal mouse calvaria [24], was purchased from RIKEN Cell Bank (Tsukuba, Japan). MC3T3-E1 cells were cultured in α-MEM supplemented with 10% FBS. They are known to differentiate into mature osteoblasts in the course of the culture and to exhibit matrix mineralization when cultured in the presence of 5 mM β-GP and 100 μg/ml ascorbic acid [24]. MLO-A5 cells are a preosteocytic cell line established from the long bones of 14-day-old osteocalcin promoter-driven T-antigen transgenic mice [14]. MLO-A5 cells mineralize in sheets, not nodules, within 3 days of culture in the presence of β-GP and ascorbic acid and within 7 days even in the absence of these two substances.

Constructs and gene transduction

The recombinant adenovirus vector carrying β-galactosidase gene (AxLacZ) was kindly provided by Dr. Izumu Saito (Institute of Medicine, The University of Tokyo). The recombinant adenovirus vector carrying the dominant negative *ras* gene (Ser17 to Asn, $AxRas^{DN}$) or constitutively active *mek*1 gene (Ser218 and Ser222 to Glu, $AxMek^{CA}$) under the control of CAG [cytomegalovirus (CMV) immediate early (IE) enhancer+chicken β-actin promoter+rabbit β-globin poly (A) signal] promoter was provided by Dr. Hideki Katagiri (Tohoku University) [20], and *runx2* gene was by Toshihisa Komori (Nagasaki University) [8]. The efficiency of infection is affected not only by the concentration of viruses and cells, but also by the ratio of the former to the latter, the multiplicity of infection (MOI). Infection of the cells by adenovirus vectors was carried out as described.

Immunoblotting

All the extraction procedures were performed at 4°C or on ice. Cells were washed with PBS and then lysed by adding TNE buffer (1% NP-40, 10 mM Tris–Hcl, pH 7.8, 150 mM NaCl, 1 mM EDTA, 2 mM Na_3VO_4, 10 mM NaF and 10 μg/ml aprotinin). The lysates were prepared by centrifugation at 15,000× rpm for 20 min. An equal amount (15 μg) of proteins was electrophoresed on 10% SDS polyacrylamide gels. After electrophoresis, proteins were electronically transferred onto a nitrocellulose membrane. Immunoblotting with specific antibodies was carried out using ECL Western blotting reagents (Amersham Co., IL, USA) according to the conditions recommended by the supplier.

MTT [3-(4,5-dimethyl-2-thiazolyl)-2,5-diphenyl-2H tetrazolium bromide] assay

After viral infection for 2 days, cells were replated on 96 well plates at the density of 5000 cells/well and incubated in 10 μl MTT solution (5 mg/ml in PBS) for 4 h. After incubation, 100 μl of 0.04 M HCl/isopropanol solution was added to melt the formazan crystal. The OD values were read at 570 nm wavelength. The cell proliferation indices were calculated by the OD value in adenovirus wells (cells plus adenoviruses) divided by the OD value in control wells (cells only), and then multiplied by 100.

Histocytochemistry

Cultures were fixed with 99% ethanol and subjected to Alizarin Red staining to assess matrix mineralization. In brief, cells were immersed in Alizarin Red solution (1% at pH 6.4) for 2 min at room temperature, and nonspecific staining was removed by several washes in distilled water.

Total RNA extraction and real time PCR

Total RNA was isolated from cultured cells with ISOGEN (Wako) following the supplier's protocol. Complementary DNA (cDNA) was synthesized from 1 μg of total RNA using the SUPERSCRIPT II reverse transcriptase kit (Invitrogen, CA, USA). For real time PCR, ABI Prism Sequence Detection System 7000 was used. Primers were designed based on Genbank, and amplicons of 50–250 base pairs with T_m between 55 and 60°C were selected. Aliquots of first-strand cDNA (1 μg) were amplified using QuantiTect SYBER Green PCR Kit (Qiagen, CA, USA) under the following conditions: initial denaturation for 10 min at 94°C followed by 40 cycles of 15 s at 94°C and 1 min at 60°C. Data analysis consisted of fold induction, and expression ratio was calculated from differences in threshold cycles at which an increase in reporter fluorescence above a baseline signal was first detected among three samples and then averaged for duplicate experiments. The primers we utilized in real time PCR to detect ALP, OCN, osteopontin (OPN), bone sialoprotein (BSP), type I collagen (Col I) and β-actin were as follows:

ALP	5′-GCTGATCATTCCCACGTTTT-3′
	5′-CTGGGCCTGGTAGTTGTTGT-3′
OCN	5′-AAGCAGGAGGGCAATAAGGT-3′
	5′-TTTGTAGGCGGTCTTCAAGC-3′
OPN	5′-ACACTTTCACTCCAATCGTCC-3′
	5′-TGCCCTTTCCGTTGTTGTCC-3′
BSP	5′-CAGAGGAGGCAAGCGTCACT-3′
	5′-CTGTCTGGGTGCCAACACTG-3′
Col I	5′-ACGTCCTGGTGAAGTTGGTC-3′
	5′-CAGGGAAGCCTCTTTCTCCT-3′
ANK	5′-CTGCTGCTACAGAGGCAGTG-3′
	5′-ACAAGGCTGGTGATGAGGAC-3′
PC-1	5′-TGAGAAGAGGCTGTCCAGGT-3′
	5′-AGTATGTGCCGGACTTGACC-3′
β-actin	5′-AGATGTGGATCAGCAAGCAG-3′
	5′-GCGCAAGTTAGGTTTTGTCA-3′

In vivo mineralization assay

Fifty microliters of adenovirus vectors containing approximately 2.5×10^7 virus particles or normal saline was injected onto the calvaria of 1-day-old ddY mice using a microinjector. Five days after the injection, the mice were sacrificed and the calvaria were removed, and paraffin-embedded sections of the calvaria were subjected to Alizarin Red staining. To analyze the efficiency of the adenovirus infection, calvaria from AxLacZ-injected mice were subjected to X-gal staining.

Results

MLO-A5 cells were positively stained with Alizarin Red after 3 days of culture in the presence of β-GP and ascorbic acid, and 7 days even in the absence of these reagents, demonstrating the strong mineralization activity of the cells (Fig. 1A) [14]. Mineralization of the cells was strongly promoted by Mek inhibitor PD98059, which dose-dependently suppressed Erk activity in the cells as determined by Western blotting with anti-phospho-Erk antibody (Fig. 1B). PDGF is a member of the PDGF/VEGF (vascular endothelial growth factor) family, which binds to its specific receptor PDGFR belonging to the receptor-type tyrosine kinase family and activates the Ras-Raf-Mek-Erk pathway [25,26]. Treatment of MLO-A5 cells with PDGF-BB dose-dependently stimulated Erk pathways and strongly suppressed mineralization of the cells even in the presence of β-GP and ascorbic acid (Fig. 2A). Mineralization of the cells was restored by the addition of PD98059 together with PDGF, indicating that the inhibitory action of PDGF is mainly mediated through Erk activation (Fig. 2B). We further investigated the role of Erk pathways in mineralization of MLO-A5 cells using the adenovirus vector-mediated gene transduction system. MLO-A5 cells were infected with AxLacZ to determine the efficiency of adenovirus vector-mediated gene transduction. As shown in Fig. 3A, strong

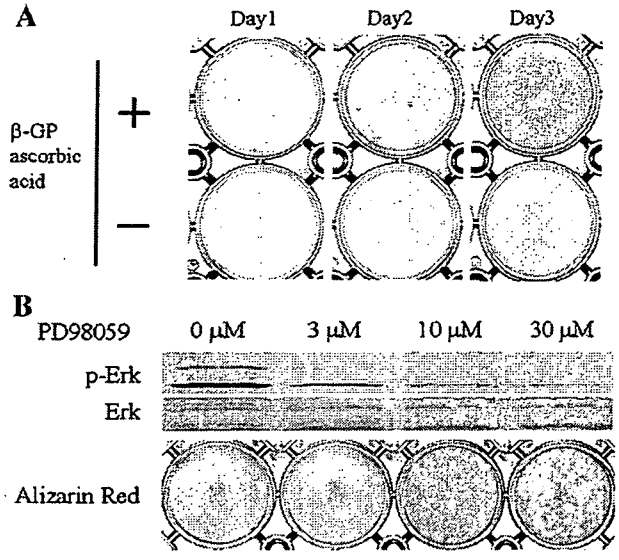

Fig. 1. Effect of matrix mineralization of MLO-A5 cell cultures by Mek inhibitor PD98059. (A) Alizarin Red staining of MLO-A5 preosteocytic cell cultures. In the presence of 5 mM β-GP and 100 μg/ml ascorbic acid, MLO-A5 cells are mineralized in 3 days as determined by Alizarin Red staining (upper column). Slight induction of mineralization was observed even in the absence of β-GP and ascorbic acid. (B) Dose-dependent inhibition of Erk activity as determined by anti-phospho-Erk Western blotting (upper column) and promotion of mineralization (lower column) in MLO-A5 cells by Mek inhibitor PD98059 on the 7th day of culture. No apparent change in the Erk expression was observed (middle column).

X-gal staining was observed in the cells infected with AxLacZ, and more than 95% of the cells were positively stained at MOI 100 with no apparent morphological changes or toxic effects. We next examined the effect of AxMek^{CA} and AxRas^{DN} on the mineralization of MLO-A5 cells. AxMek^{CA} infection induced phospho-Erk expression in the cells and strongly suppressed their mineralization, while AxRas^{DN} infection downregulated Erk phosphorylation and promoted mineralization as shown in Fig. 3B. This was not due to the effect on the cell viability since no significant change in MTT assay was observed by the viruses (Fig. 3C). AxRas^{DN} expression recovered the mineralization of MLO-A5 cells suppressed by PDGF treatment (Fig. 2C).

MC3T3-E1 is a cell line with preosteoblastic phenotypes, which differentiates into mature osteoblasts and exhibits mineralization during culture [24]. MC3T3-E1 cells were also efficiently infected by adenovirus vectors as determined by AxLacZ infection and X-gal staining (Fig. 3A). As shown in Fig. 3D, adenovirus vector-mediated *runx2* gene expression strongly upregulates the mineralization of the cells, and matrix mineralization was suppressed by AxMek^{CA} infection and promoted by AxRas^{DN} infection (Fig. 3D). These results suggest that Erk activation is a negative regulator of the mineralization independent of Runx2.

To investigate the molecular mechanism underlying the effect of Erk on MLO-A5 cells, we analyzed the osteoblastic gene expression in the cells. As shown in Fig. 4, significant increase in OPN gene expression was observed in AxMek^{CA}-infected cells compared to AxLacZ-infected cells (1.97-fold), and the gene expression was suppressed by Ras^{DN} expression (0.8-fold). ALP gene expression was significantly increased by AxRas^{DN} infection but was not affected by AxMek^{CA}. OCN gene expression was significantly decreased by AxRas^{DN} infection and increased by AxMek^{CA} but with no statistical significance. BSP and Col I gene expression was suppressed by AxMek^{CA} and increased by AxRas^{DN} without statistical significance (Fig. 4). AxMEK^{CA} infection also increased OPN expression in MC3T3-E1 cells expressing *runx2*, while no significant reduction in the expression was observed in AxRas^{DN}-infected cells (Fig. 4). We also analyzed the expression of plasma cell membrane glycoprotein 1 (PC-1) and ANK, which are known to regulate the accumulation of extracellular inorganic pyrophosphate. AxMEK^{CA} infection significantly decreased the expression of both PC-1 and ANK in MLO-A5 cells, while no significant change was observed in AxRas^{DN}-infected cells (Fig. 4).

We finally examined the effect of Erk activation in the mineralization in vivo. When AxLacZ was injected onto the calvaria of 1-day-old mice, strong X-gal staining was observed after 3 days of the injection, indicating an effective gene transduction by the adenovirus in vivo. Alizarin Red staining

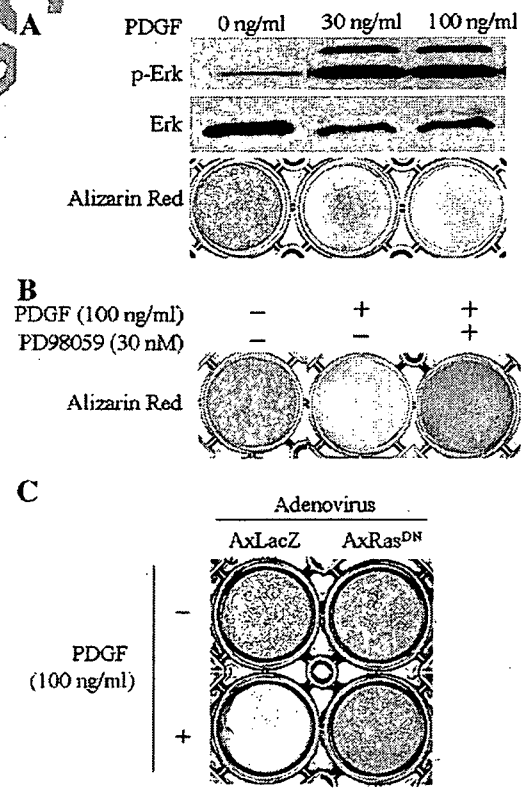

Fig. 2. Effect of PDGF-BB on mineralization of MLO-A5 cells. (A) PDGF-BB dose-dependently increased Erk activity in MLO-A5 cells as determined by phospho-Erk blotting (upper column) and promoted their mineralization (lower column). No apparent change in the Erk expression was observed (middle column). (B) Mek inhibitor PD98059 at 30 μM recovered the mineralization of MLO-A5 cells even in the presence of PDGF-BB on the 7th day of culture. (C) Inhibition of Erk pathways by dominant negative Ras adenovirus (AxRas^{DN}) recovered mineralization of MLO-A5 cells suppressed by PDGF-BB.

exhibited a decreased mineralization by AxMek^{CA} and an increased mineralization by AxRas^{DN} 5 days after the injection (Fig. 5).

Discussion

Research on the regulatory mechanism of osteoblast differentiation was remarkably advanced by the recent finding of critical transcription factors such as Runx2 and Osterix [7,9,15,21,27]. Matrix mineralization is a final step of osteoblast differentiation and plays a critical role in maintaining the mechanical integrity of the calcified tissues [2,9,17]. Defective mineralization is observed in various pathological conditions such as rickets and osteomalacia, in which bone strength is greatly reduced [3,18]. However, molecular events leading to the matrix mineralization still remain unclear. Erk pathways are essentially involved in various aspects of physiological and pathological events and regulate proliferation and differentiation of the cells [4,5,23]. In the present study, we tried to elucidate the role of these pathways on the matrix mineralization by osteogenic cells. Several previous studies attempted to clarify the role of Erk pathways on osteoblast differentiation with different and partly contradictory results. Consistent with our results, Higuchi et al. demonstrated that the Erk inhibitor PD98059 promoted the early osteoblastic differentiation and mineralization in C2C12 pluripotent mesenchymal cells treated with BMP-2 and MC3T3-E1 cells [10]. In addition, Chaudhary and Avioli reported that Erk activation by PDGF-BB or fibroblast growth factor-2 suppressed type I collagen expression in MC3T3-E1 cells, and the inhibition of Erk pathways either by specific inhibitors or by culturing the cells in low serum (0.3%) markedly increased it [6], and Nakayama et al. further reported that Erk activation negatively regulates osteoblast differentiation induced by BMP-2 [22]. On the other hand, Jaiswal reported that osteogenic medium activates Erk pathways in human mesenchymal stem cells and that the inhibition of Erk activity suppressed their osteoblastic differentiation and mineralization, indicating a positive regulatory role for Erk pathways on mineralization [13]. Lai et al. also reported that

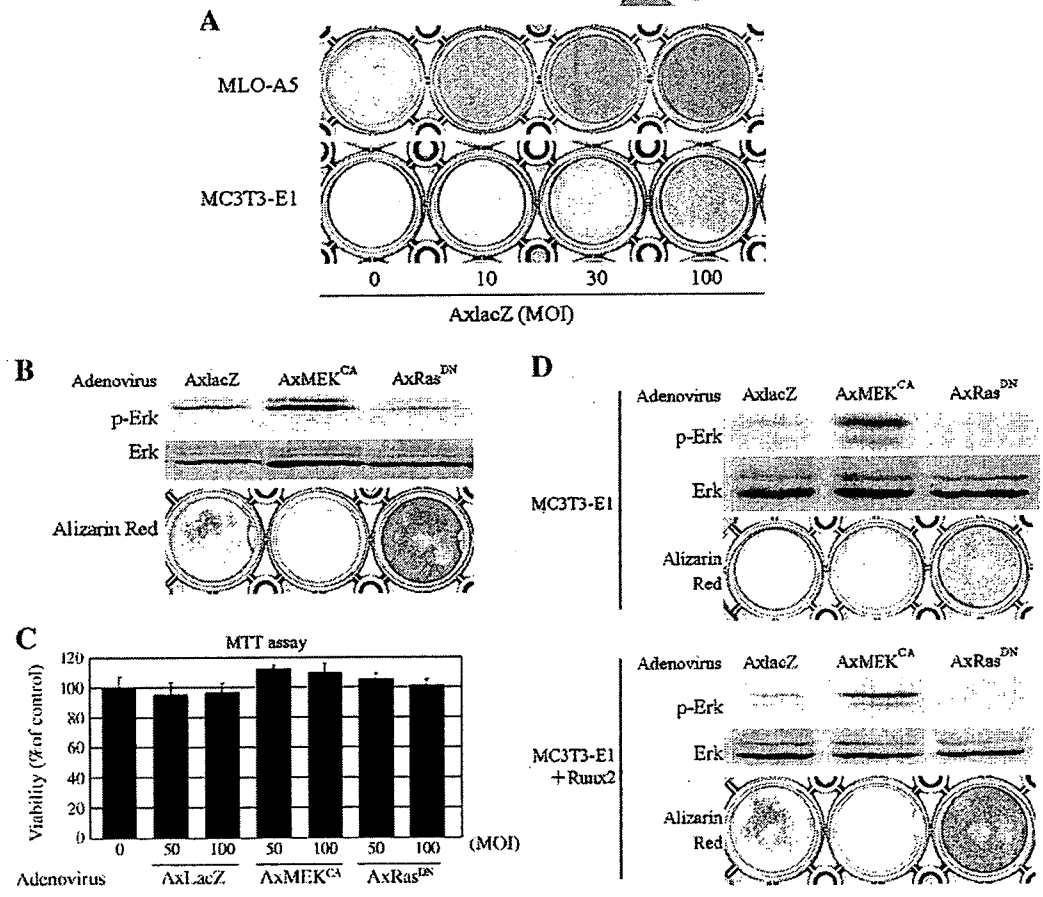

Fig. 3. Regulation of Erk pathways by adenovirus vector-mediated gene transduction system. (A) X-gal staining after 2 days of AxLacZ infection. AxLacZ efficiently and dose-dependently transduced β-galactosidase gene in MLO-A5 cells (upper) and MC3T3-E1 cells (lower). (B) Activation of Erk pathways by AxMek^{CA} infection suppressed and their inhibition by AxRas^{DN} infection promoted the matrix mineralization of MLO-A5 cells on the 7th day of culture. (C) MTT assay. Neither infection of AxMek^{CA} nor AxRas^{DN} affected the viability of MLO-A5 cells. No significant difference was observed between adenovirus-infected cultures and control cultures. (D) Effect of AxMek^{CA} and AxRas^{DN} infection on Erk activation and matrix mineralization of MC3T3-E1 cells (upper) and MC3T3-E1 cells overexpressing Runx2 (lower).

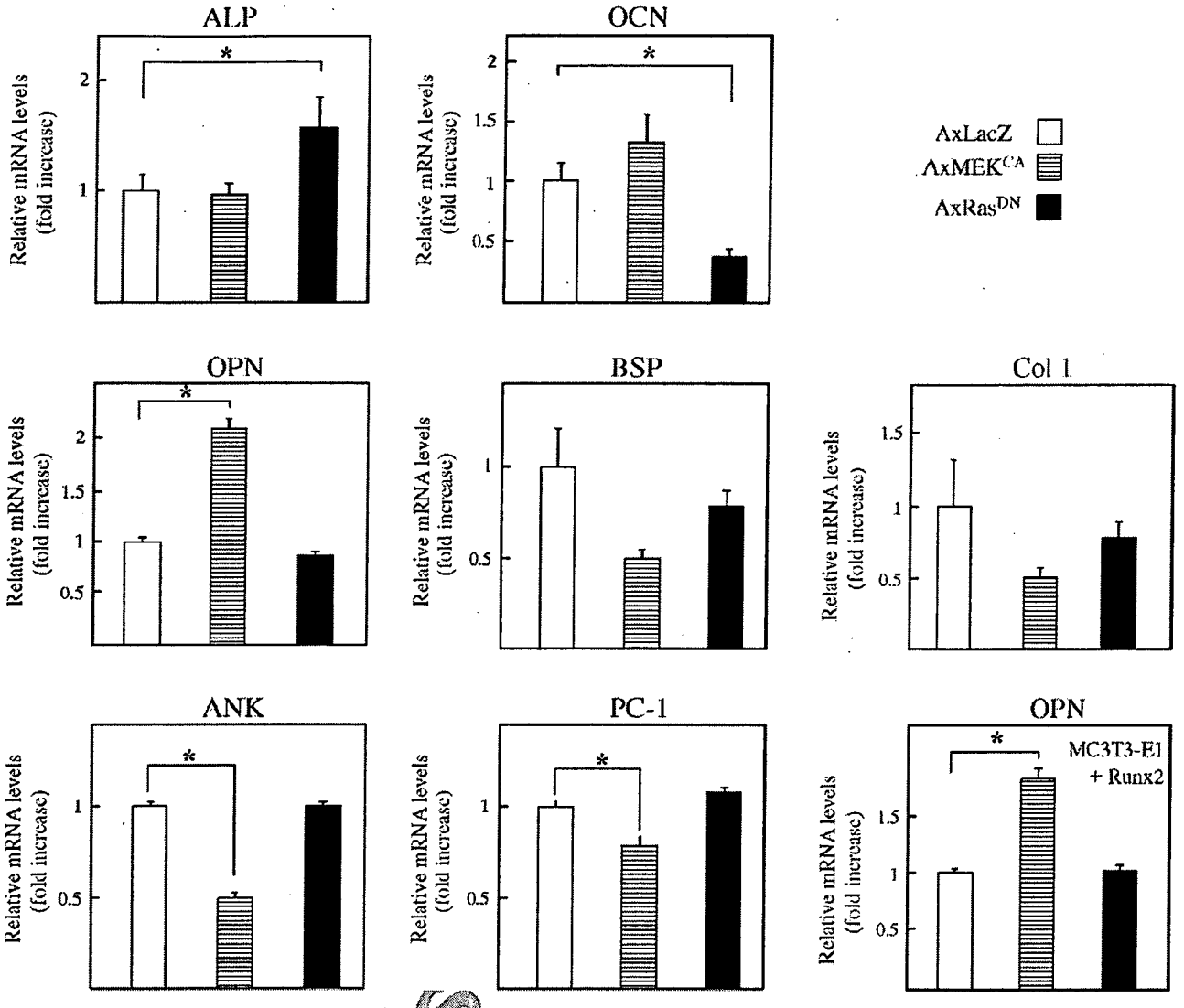

Fig. 4. Real time PCR analysis. Effect of AxMek^{CA} and AxRas^{DN} infection on mRNA levels of ALP, OCN, OPN, BSP, Col I, PC-1 and ANK was determined by real time PCR after 2 days of infection in MLO-A5 cells. Effects of these adenoviruses on OPN mRNA expression were also examined in MC3T3-E1 cells overexpressing *runx2* gene. *Significantly different from AxLacZ-infected cells, $p<0.05$.

inhibition of Erk activity by expressing dominant negative Erk1 suppressed osteoblast differentiation and matrix mineralization by reducing ALP activity and the deposition of bone matrix proteins [16]. These contradictory results are at least partly due to the difficulty in examining the mineralization process independently of the osteoblast differentiation.

Using preosteocytic cell line MLO-A5 cells and osteoblastic MC3T3-E1 cells, we investigated the direct role of Erk pathways on the mineralization process. MLO-A5 cells are known to mineralize even without β-GP or ascorbic acid, and treating the cells with Mek inhibitor PD98059 stimulated mineralization (Fig. 1), while PDGF treatment, which strongly stimulates these pathways, suppressed it (Fig. 2A). The inhibitory effect of PDGF was reversed by PD98059 or AxRas^{DN} infection, indicating a critical involvement of Erk pathways (Figs. 2B and C). Direct activation of Erk pathways by adenovirus vector-mediated Mek^{CA} expression suppressed the mineralization of MLO-A5 cells, and inhibition of the pathways by Ras^{DN} expression increased it. Overexpression of Runx2 markedly promoted the terminal differentiation and mineralization of osteoblastic MC3T3-E1 cells, while Mek^{CA} expression suppressed and Ras^{DN} expression promoted their mineralization. Similar effects of these viruses were observed in primary osteoblasts (data not shown). Importantly, Erk activity regulates the skeletal mineralization in vivo as well. Injecting AxMek^{CA} onto the calvaria of 1-day-old mice suppressed, while AxRas^{DN} injection promoted the mineralization of calvaria. These results suggest that the Erk activation negatively regulates mineralization of osteoblasts or osteocytes not only in vitro but also in vivo, although the effect of the viruses on other types of cells cannot be ruled out. The exact regulatory mechanism of mineralization by Erk pathways still remains unclear. We found that Erk activation significantly increased OPN expression in MLO-A5 cells. Using an in vitro mineralization assay system,

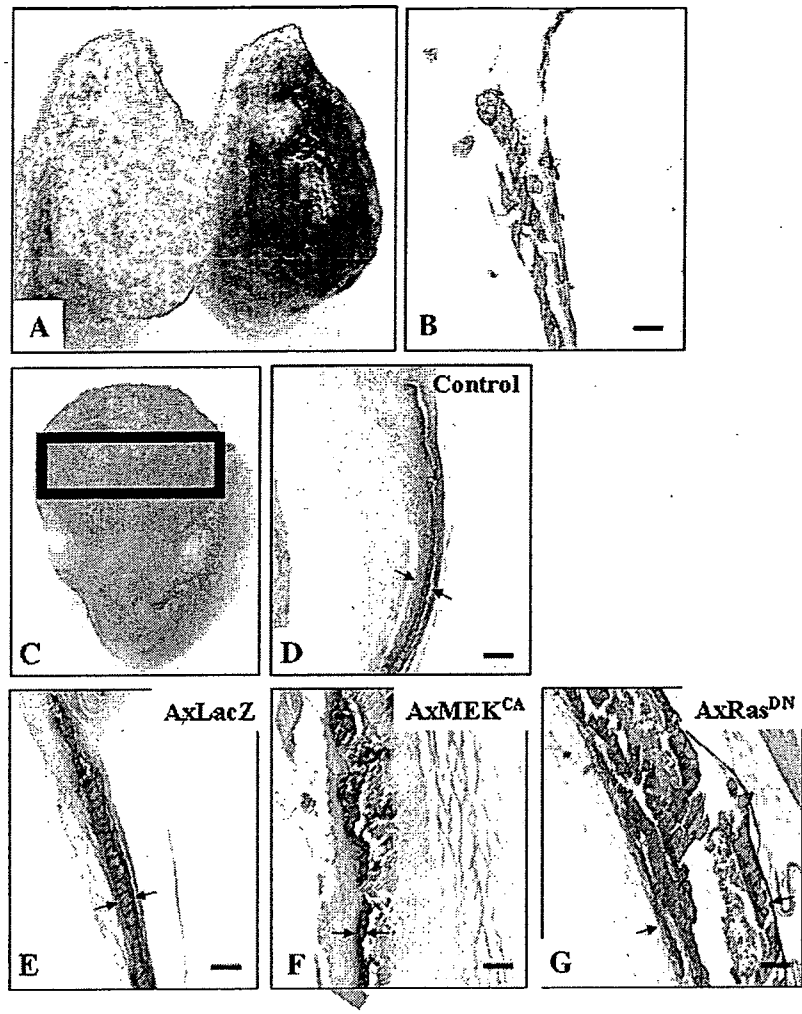

Fig. 5. In vivo mineralization assay. (A) X-gal staining of mouse calvaria injected with either normal saline (left) or AxLacZ (right). (B) Histological analysis of AxLacZ-injected mouse calvaria stained for β-galactosidase activity. (C–G) Normal saline (D), AxLacZ (E), AxMek^{CA} (F) or AxRas^{DN} (G) was injected onto the calvaria of 1-day-old ddY mice. Five days after the injection, mice were sacrificed and the rectangular areas of the calvaria (C) were subjected to Alizarin Red staining. Experiments were repeated four times with almost the same results, and representative pictures are shown. Arrows indicate the thickness of the calvaria. Scale bars=100 μm.

Hunter et al. demonstrated that OPN suppressed hydroxyapatite formation and that treatment of OPN with ALP reduced its mineralization-inhibitory activity [11,12]. Therefore, it is possible that Erk pathways regulate the mineralization of osteoblasts/osteocytes by regulating OPN expression in the cells. Experiments using OPN deficient mice will clarify the role of the molecule in the mineralization process in the future. We also found that MEK^{CA} expression significantly reduced the expression of PC-1 and ANK in MLO-A5 cells. These molecules are known to regulate the accumulation of extracellular inorganic pyrophosphate and may affect the mineralization of the cells. Further studies are required to elucidate the regulatory mechanism of mineralization through Ras-Erk pathways.

In summary, we found that the Erk pathway is a negative regulator of skeletal mineralization both in vitro and in vivo. Therapeutics targeting Erk pathways can promote bone strength and bone quality by modulating matrix mineralization.

Acknowledgments

The authors thank R. Yamaguchi (Department of Orthopaedic Surgery, The University of Tokyo), who provided expert technical assistance. AxLacZ was kindly provided by Izumu Saito (Institute of Medicine, The University of Tokyo), AxMek^{CA} and AxRas^{DN} by Hideki Katagiri (Tohoku University) and AxRunx2 by Toshihisa Komori (Nagasaki University). This work was in part supported by Grants-in-Aid from the Ministry of Education, Culture, Sports, Science and Technology of Japan and by Health Science research grants from the Ministry of Health and Welfare of Japan.

References

[1] Aarden EM, Burger EH, Nijweide PJ. Function of osteocytes in bone. J Cell Biochem 1994;55:287–99.

[2] Aubin JE, Liu F, Malaval L, Gupta AK. Osteoblast and chondroblast differentiation. Bone 1995;17:77S–83S.
[3] Berry JL, Davies M, Mee AP. Vitamin D metabolism, rickets, and osteomalacia. Semin Musculoskelet Radiol 2002;6:173–82.
[4] Bourne HR, Sanders DA, McCormick F. The GTPase superfamily: Conserved structure and molecular mechanism. Nature 1991;349:117–27.
[5] Campbell SL, Khosravi-Far R, Rossman KL, Clark GJ, Der CJ. Increasing complexity of Ras signaling. Oncogene 1998;17:1395–413.
[6] Chaudhary LR, Avioli LV. Extracellular-signal regulated kinase signaling pathway mediates downregulation of type I procollagen gene expression by FGF-2, PDGF-BB, and okadaic acid in osteoblastic cells. J Cell Biochem 2000;76:354–9.
[7] Ducy P, Zhang R, Geoffroy V, Ridall AL, Karsenty G. Osf2/Cbfa1: A transcriptional activator of osteoblast differentiation. Cell 1997;89:747–54.
[8] Fujita T, Azuma Y, Fukuyama R, Hattori Y, Yoshida C, Koida M, et al. Runx2 induces osteoblast and chondrocyte differentiation and enhances their migration by coupling with PI3K-Akt signaling. J Cell Biol 2004;166:85–95.
[9] Harada S, Rodan GA. Control of osteoblast function and regulation of bone mass. Nature 2003;423:349–55.
[10] Higuchi C, Myoui A, Hashimoto N, Kuriyama K, Yoshioka K, Yoshikawa H, et al. Continuous inhibition of MAPK signaling promotes the early osteoblastic differentiation and mineralization of the extracellular matrix. J Bone Miner Res 2002;17:1785–94.
[11] Hunter GK, Hauschka PV, Poole AR, Rosenberg LC, Goldberg HA. Nucleation and inhibition of hydroxyapatite formation by mineralized tissue proteins. Biochem J 1996;317(Pt 1):59–64.
[12] Hunter GK, Kyle CL, Goldberg HA. Modulation of crystal formation by bone phosphoproteins: structural specificity of the osteopontin-mediated inhibition of hydroxyapatite formation. Biochem J 1994;300(Pt 3):723–8.
[13] Jaiswal RK, Jaiswal N, Bruder SP, Mbalaviele G, Marshak DR, Pittenger MF. Adult human mesenchymal stem cell differentiation to the osteogenic or adipogenic lineage is regulated by mitogen-activated protein kinase. J Biol Chem 2000;275:9645–52.
[14] Kato Y, Boskey A, Spevak L, Dallas M, Hori M, Bonewald LF. Establishment of an osteoid preosteocyte-like cell MLO-A5 that spontaneously mineralizes in culture. J Bone Miner Res 2001;16:1622–33.
[15] Komori T, Yagi H, Nomura S, Yamaguchi A, Sasaki K, Deguchi K, et al. Targeted disruption of Cbfa1 results in a complete lack of bone formation owing to maturational arrest of osteoblasts. Cell 1997;89:755–64.
[16] Lai CF, Chaudhary L, Fausto A, Halstead LR, Ory DS, Avioli LV, et al. Erk is essential for growth, differentiation, integrin expression, and cell function in human osteoblastic cells. J Biol Chem 2001;276:14443–50.
[17] Lynch MP, Stein JL, Stein GS, Lian JB. The influence of type I collagen on the development and maintenance of the osteoblast phenotype in primary and passaged rat calvarial osteoblasts: modification of expression of genes supporting cell growth, adhesion, and extracellular matrix mineralization. Exp Cell Res 1995;216:35–45.
[18] Mankin HJ. Rickets, osteomalacia, and renal osteodystrophy. An update. Orthop Clin North Am 1990;21:81–96.
[19] Mikuni-Takagaki Y. Mechanical responses and signal transduction pathways in stretched osteocytes. J Bone Miner Metab 1999;17:57–60.
[20] Miyazaki T, Katagiri H, Kanegae Y, Takayanagi H, Sawada Y, Yamamoto A, et al. Reciprocal role of ERK and NF-kappaB pathways in survival and activation of osteoclasts. J Cell Biol 2000;148:333–42.
[21] Nakashima K, Zhou X, Kunkel G, Zhang Z, Deng JM, Behringer RR, et al. The novel zinc finger-containing transcription factor osterix is required for osteoblast differentiation and bone formation. Cell 2002;108:17–29.
[22] Nakayama K, Tamura Y, Suzawa M, Harada S, Fukumoto S, Kato M, et al. Receptor tyrosine kinases inhibit bone morphogenetic protein-Smad responsive promoter activity and differentiation of murine MC3T3-E1 osteoblast-like cells. J Bone Miner Res 2003;18:827–35.
[23] Su B, Karin M. Mitogen-activated protein kinase cascades and regulation of gene expression. Curr Opin Immunol 1996;8:402–11.
[24] Sudo H, Kodama HA, Amagai Y, Yamamoto S, Kasai S. In vitro differentiation and calcification in a new clonal osteogenic cell line derived from newborn mouse calvaria. J Cell Biol 1983;96:191–8.
[25] Ullrich A, Schlessinger J. Signal transduction by receptors with tyrosine kinase activity. Cell 1990;61:203–12.
[26] Williams LT. Signal transduction by the platelet-derived growth factor receptor. Science 1989;243:1564–70.
[27] Yamaguchi A, Komori T, Suda T. Regulation of osteoblast differentiation mediated by bone morphogenetic proteins, hedgehogs, and Cbfa1. Endocr Rev 2000;21:393–411.

Mod Rheumatol (2007) 17:17–23
DOI 10.1007/s10165-006-0531-1

ORIGINAL ARTICLE

**Ayako Suematsu · Yasuhito Tajiri · Tomoki Nakashima
Junko Taka · Sae Ochi · Hiromi Oda · Kozo Nakamura
Sakae Tanaka · Hiroshi Takayanagi**

Scientific basis for the efficacy of combined use of antirheumatic drugs against bone destruction in rheumatoid arthritis

Received: October 13, 2006 / Accepted: October 18, 2006

Abstract Finding a means to ameliorate and prevent bone destruction is one of the urgent issues in the treatment of rheumatoid arthritis. Recent studies revealed bone-resorbing osteoclasts to be essential for arthritic bone destruction, but to date there has been scarce experimental evidence for the underlying mechanism of the bone-protective effect of antirheumatic drugs. Here we examined the effects of one or a combination of disease-modifying antirheumatic drugs (DMARDs) on osteoclast differentiation to provide a cellular and molecular basis for their efficacy against bone destruction. The effects on osteoclast precursor cells and osteoclastogenesis-supporting cells were distinguished by two in vitro osteoclast culture systems. Methotrexate (MTX), bucillamine (Buc) and salazosulphapyridine (SASP) inhibited osteoclastogenesis by acting on osteoclast precursor cells and interfering with receptor activator of NF-κB ligand (RANKL)-mediated induction of the nuclear factor of activated T cells (NFAT) c1. MTX and SASP also suppressed RANKL expression on osteoclastogenesis-supporting mesenchymal cells. Interestingly, the combination of three antirheumatic drugs exerted a marked inhibitory effect on osteoclastogenesis even at a low dose at which there was much less of an effect when administered individually. These results are consistent with the reported efficacy of combined DMARDs therapy in humans and suggest that osteoclast culture systems are useful tools to provide an experimental basis for the bone-protective effects of antirheumatic drugs.

Key words Disease-modifying antirheumatic drugs (DMARDs) · Nuclear factor of activated T cells (NFAT) c1 · Osteoclast · Receptor activator of NF-κB ligand (RANKL) · Rheumatoid arthritis (RA)

A. Suematsu · T. Nakashima · J. Taka · S. Ochi · H. Takayanagi (✉)
Department of Cell Signaling, Graduate School, Tokyo Medical and Dental University and COE Program for Frontier Research on Molecular Destruction and Reconstruction of Tooth and Bone, 1-5-45 Yushima, Bunkyo-ku, Tokyo 113-8549, Japan
Tel. +81-3-5803-5471; Fax +81-3-5803-0192
e-mail: taka.csi@tmd.ac.jp

Y. Tajiri · K. Nakamura · S. Tanaka
Department of Orthopaedic Surgery, Graduate School of Medicine, University of Tokyo, Tokyo, Japan

H. Oda
Department of Orthopaedic Surgery, Saitama Medical University, Saitama, Japan

H. Takayanagi
Solution-Oriented Research for Science and Technology (SORST), Japan Science and Technology Agency (JST), Kawaguchi, Japan

Introduction

Rheumatoid arthritis (RA) is an autoimmune disease characterized by the chronic inflammation of synovial joints which results in severe bone destruction.[1,2] A number of anti-inflammatory and antirheumatic drugs have been clinically utilized in the treatment of RA, but there is no method to prevent bone destruction completely.[3,4] This is partly because all the antirheumatic drugs were originally developed to suppress the activation of the immune system.[5] However, a combined use of disease-modifying antirheumatic drugs (DMARDs) has considerably contributed to the amelioration of both inflammation and bone destruction, although the effects are still not fully satisfactory.[6–8] It is poorly understood how the antirheumatic drugs exert their bone-protective effects, and it has thus been extremely difficult to predict the efficacy of antirheumatic drugs against bone destruction based on in vitro experiments.

Osteoclasts are multinucleated cells of monocyte/macrophage lineage that resorb bone matrix.[9,10] The generation of osteoclasts is supported by mesenchymal cells such as osteoblasts, which provide signals essential for differentiation.[11] These signals are mediated by macrophage colony-stimulating factor (M-CSF), receptor activator of NF-κB ligand (RANKL), and costimulatory signals for RANKL.[12–16] For the evaluation of osteoclast formation, two types of in vitro osteoclast differentiation systems have been developed: osteoclast precursor cells, bone marrow-derived monocyte/macrophage lineage cells (BMMs), which are stimulated with recombinant RANKL and M-CSF (the

RANKL/M-CSF system, Fig. 1a), or are cocultured with osteoblasts in the presence of 1,25-$(OH)_2$ vitamin D_3 ($VitD_3$) and prostaglandin E_2 (PGE_2) (the coculture system, Fig. 2a). The RANKL/M-CSF system is suitable for looking at the direct effect of drugs on the osteoclast precursor cells and RANKL-induced signaling events.[17,18] The coculture system is useful in the investigation of the effect of drugs on the osteoclastogenesis-supporting cells and the expression of osteoclastogenic factors such as RANKL.[19]

Osteoclasts are abundantly observed at the bone/synovium interface in the joints of RA patients.[2,20,21] RANKL is highly expressed by synovial fibroblasts in arthritic joints and is responsible for the abnormal activation of osteoclasts.[22,23] Importantly, arthritic bone destruction is greatly reduced in *RANKL*$^{-/-}$ mice or *Fos*$^{-/-}$ mice, both of which lack osteoclasts, even though there is no significant difference in the level of inflammation between the wild type and these genetically modified mice.[24,25] Consistent with this, anti-osteoclast therapy has successfully ameliorated bone damage in models of inflammatory bone destruction.[26–28] Thus, accumulating evidence indicates that bone destruction in RA is attributable to the abnormal activation of osteoclasts and that inhibition of RANKL-mediated osteoclastogenesis may be an ideal method to control arthritic bone destruction.[1,3,12]

Methotrexate (MTX), a folate antagonist, is an antirheumatic drug widely used in the world, often in combination with other drugs such as salazosulphapyridine (SASP).[6,7,29] Bucillamine (Buc), *N*-(2-mercapto-2-methylpropionyl)-L-cysteine, is used clinically in Japan and Korea to treat patients with RA.[30–32] Buc has structural similarities to D-penicillamine, but contains two free sulfhydryl groups, resulting in molecular and therapeutic effects significantly different from D-penicillamine.[32] Here we examined the effect of MTX, Buc and SASP on the osteoclast differentiation using two mouse in vitro osteoclast formation systems and found that the three drugs exerted inhibitory effects on osteoclastogenesis by differentially acting on osteoclast precursor and osteoclastogenesis-supporting cells. Even though the effect of a low dose of the drugs administered individually was small, in combination they had a marked inhibitory effect on osteoclastogenesis through a downregulation of nuclear factor of activated T cells (NFAT) c1 induction. Thus, the analysis of the effect of antirheumatic drugs on in vitro osteoclast differentiation may provide a crucial clue on their capacity to protect against bone destruction.

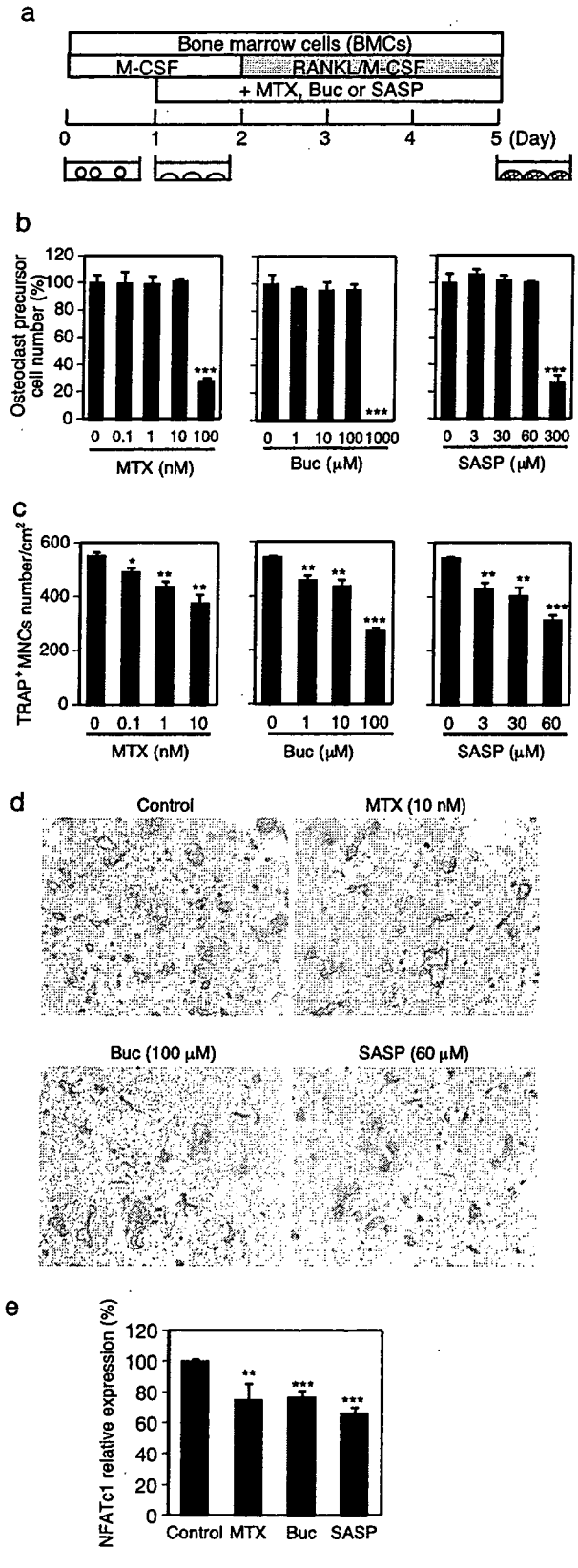

Fig. 1. Effects of methotrexate (*MTX*), bucillamine (*Buc*) and salazosulphapyridine (*SASP*) on receptor activator of NF-κB ligand (*RANKL*)-induced osteoclastogenesis. **a** A schematic of the osteoclast formation system induced by RANKL and macrophage-colony stimulating factor (*M-CSF*) (the RANKL/M-CSF system). **b** Effects of MTX, Buc, and SASP on the cell number of osteoclast precursor cells. Bone marrow-derived monocyte/macrophage lineage cells (BMMs) were treated with MTX, Buc, or SASP in the presence of M-CSF. Four days later, the number of osteoclast precursor cells was estimated microscopically. **c** Effect of MTX, Buc, or SASP on osteoclastogenesis in the RANKL/M-CSF system. **d** Microscopic photographs of RANKL-induced osteoclastogenesis in the presence of MTX, Buc or SASP (TRAP staining). **e** Expression of *NFATc1* protein in RANKL-stimulated BMMs treated with MTX (10 nM), Buc (100 μM) or SASP (60 μM)

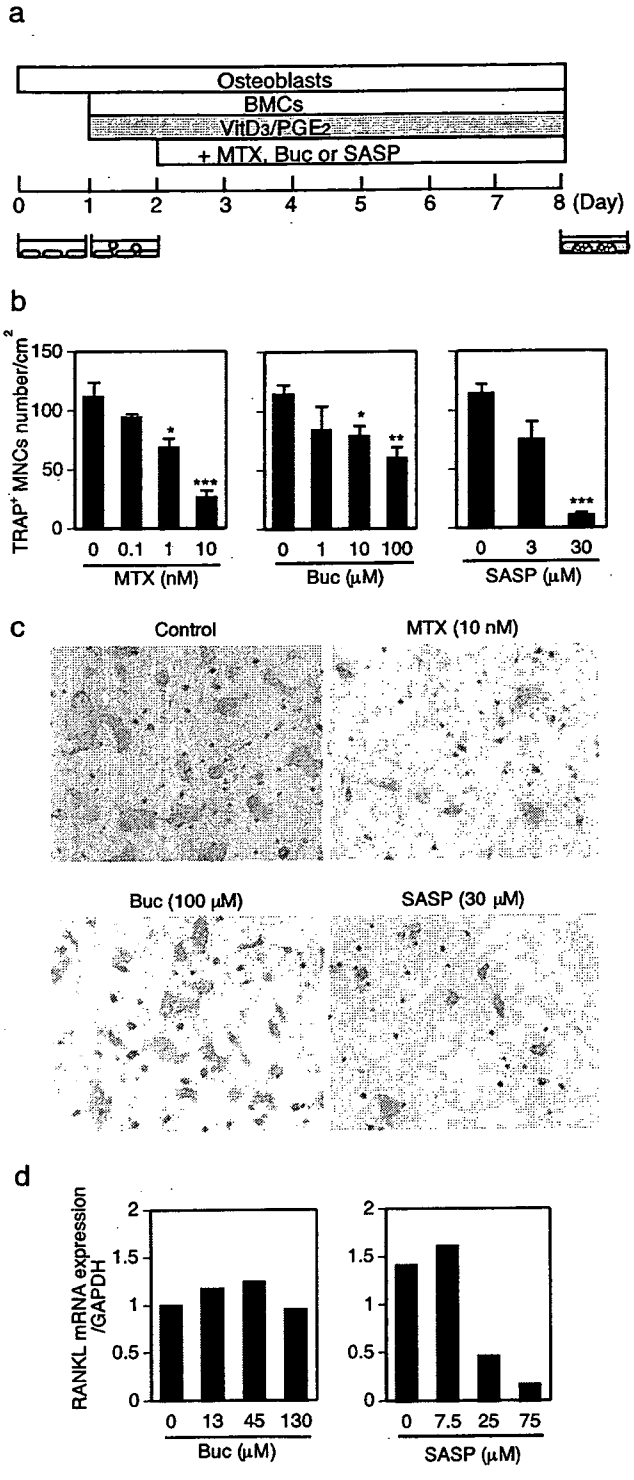

Fig. 2. Effect of methotrexate (*MTX*), bucillamine (*Buc*) and salazosulphapyridine (*SASP*) on osteoclastogenesis in the coculture system. **a** A schematic of the coculture system for osteoclastogenesis. BMCs, bone marrow cells; $VitD_3$, 1,25-$(OH)_2$ vitamin D_3; PGE_2, prostaglandin E_2. **b** Effects of MTX, Buc or SASP on osteoclastogenesis in the coculture system. **c** Microscopic photographs of osteoclastogenesis in the coculture in the presence of MTX, Buc, or SASP (TRAP staining). **d** Expression of *RANKL mRNA* in osteoblasts stimulated with Buc or SASP evaluated by reverse transcriptase-polymerase chain reaction (RT-PCR). Mouse primary osteoblasts were stimulated with $VitD_3$ in the presence of Buc or SASP for 4 days. RT-PCR analysis was repeated several times and yielded similar results; a representative set of data is shown

Materials and methods

The RANKL/M-CSF system for in vitro osteoclast formation

The method of the RANKL/M-CSF system for osteoclastogenesis was described previously,[17,33] and is here utilized with modifications (see Fig. 1a). Nonadherent bone marrow cells (BMCs) were obtained from C57BL/6 mice (6- to 8-week-old) (CLEA Japan, Tokyo, Japan) maintained under specific pathogen-free conditions. All animal experiments were performed with the approval of the Animal Study Committee of Tokyo Medical and Dental University, and conformed to recognized guidelines and laws. BMCs were seeded (2×10^5 per well in a 24-well plate), and cultured in α-MEM (Gibco, Paisly, UK) containing 10% fetal bovine serum (FBS; Sigma, St. Louis, MO, USA), 0.1 μg/ml ampicillin, 0.1 mg/ml kanamycin (Meiji Seika, Tokyo, Japan) and 10 ng/ml recombinant M-CSF (R&D Systems, Minneapolis, MN, USA) for 2 days. Adherent cells were used as BMMs after washing out the nonadherent cells including lymphocytes. These BMMs were stimulated with 50 ng/ml recombinant RANKL (PeproTech, Rocky Hill, NJ, USA) in the presence of 10 ng/ml M-CSF for additional 3 days. The treatment of BMMs with MTX, Buc or SASP (Santen Pharmaceutical, Tokyo, Japan) started 1 day before RANKL treatment and continued until the end of the culture. The medium was replaced completely every 2 days. Tartrate-resistant acid phosphatase-positive multinucleated cells ($TRAP^+$ MNCs) (>3 nuclei unless otherwise indicated) were counted.

The coculture system for in vitro osteoclast formation

The method of coculture system for osteoclastogenesis was described previously,[14,34] and utilized with modifications (see Fig. 2a). Primary osteoblasts were isolated from the calvaria of newborn (1–2 days old) mice by enzymatic digestion in α-MEM medium with 0.1% collagenase (Wako, Osaka, Japan) and 0.2% dispase (Sanko Junyaku, Tokyo, Japan) and cultured in α-MEM with 10% FBS. One day after these osteoblasts were reseeded (1×10^4 per well in a 24-well plate), BMCs (1×10^5 per well in a 24-well plate) were added to the culture of osteoblasts and cocultured in α-MEM with 10% FBS containing 1×10^{-8} M $VitD_3$ and 1×10^{-6} M PGE_2 (Wako) for 7 days. One day after BMCs were added, MTX, Buc or SASP was added to the coculture. $TRAP^+$ MNCs (>3 nuclei) were counted 7 days after addition of BMC.

Immunofluorescence staining

Cells were fixed in 4% paraformaldehyde/phosphate buffered saline (PBS) for 20 min, and treated with 0.2% Triton X-100 for 5 min. The cells were sequentially incubated in 5% bovine serum albumin/PBS for 30 min, 2 μg/ml anti-NFATc1 monoclonal antibody (7A6, Santa Cruz Biotech-

nology, Santa Cruz, CA, USA) for 60 min and then in Alexa Fluor 488-labeled secondary antibody (Molecular Probes, Eugene, OR, USA) for 60 min. The relative expression of NFATc1 was calculated by computational densitometry using NIH Image software.

RNA extraction and reverse transcriptase-polymerase chain reaction analysis

Osteoblasts isolated from mouse calvaria were reseeded (1×10^7 per well in a 10-cm dish), and cultured in α-MEM with 10% FBS containing 1×10^{-8} M $VitD_3$ in the presence of Buc (0–130 μM) or SASP (0–75 μM) for 4 days. Total RNA was extracted using ISOGEN (Nippon Gene, Tokyo, Japan) and first-strand complementary DNA (cDNA) was synthesized from total RNA using the One-Step RNA PCR kit (Takara Bio, Shiga, Japan) according to the manufacturer's protocol. The primers used for the mouse RANKL were the following: 5′-TCAGAAGACAGCACTCAGTG-3′ (sense) and 5′-TCTTCACCAGCTCGGAGCTT-3′ (antisense). The amplification protocol consisted of an initial denaturation at 94°C for 2 min, followed by 40 cycles of denaturation at 94°C for 30 s, annealing at 55°C for 30 s, and extension at 72°C for 90 s. The level of mRNA expression was normalized with that of GAPDH expression. The PCR products were subjected to electrophoresis on 1.5% agarose gels and stained with ethidium bromide, and the bands were measured by computational densitometry using NIH Image software.

Statistical analysis

All data are expressed as mean ± s.e.m ($n = 5$). Statistical analysis was performed using Student's t-test or ANOVA followed by the Bonferroni test, if applicable ($^*P < 0.05$, $^{**}P < 0.01$, $^{***}P < 0.001$, unless otherwise indicated). Results are representative examples of three or more independent experiments.

Results

The effect of antirheumatic drugs such as MTX and SASP on osteoclast formation have been described in previous reports.[35] However, these drugs have cell toxicity at high doses and it has been unclear whether the effects of these drugs have been investigated properly at concentrations that do not induce cell toxicity. Therefore, we first examined the effect of MTX, Buc, and SASP on the survival of osteoclast precursor cells, BMMs. BMMs were obtained by stimulating mouse BMCs with M-CSF, and the cell number of BMMs was counted after 4-day culture in the presence of various concentrations of MTX, Buc and SASP. All of these drugs had no effect on the cell number of BMMs at low concentrations, suggesting that they did not affect cell survival or proliferation. In contrast, they had severe toxic effects at high concentrations (Fig. 1b). Therefore, we used concentrations of the drugs (MTX: 0.1–10 nM, Buc: 1–100 μM, SASP: 3–60 μM) at which they exerted minimal effects on the cell number of BMMs. When these drugs were added to the RANKL/M-CSF system at these concentrations (Fig. 1a), all three drugs had statistically significant but mild suppressive effects on osteoclast differentiation in a dose-dependent manner, as revealed by the decreased formation of $TRAP^+$ MNCs (Fig. 1c, d).

NFATc1 is the essential transcription factor for osteoclastogenesis.[17,36] It has been shown that RANKL dramatically induces the expression of NFATc1 through an autoamplification mechanism and the level of NFATc1 determines the fate of cells of the osteoclast lineage.[36] Certain antirheumatic drugs that have bone-protective effects inhibit osteoclastogenesis by suppressing RANKL-induced NFATc1 expression.[17,20] To analyze the effects of the three antirheumatic drugs on the expression of NFATc1, we quantitated the protein level of NFATc1 in the RANKL-stimulated BMMs after immunostaining with a specific antibody against NFATc1. All three drugs had similar inhibitory effects on NFATc1 induction, although the effects were only partial (Fig. 1e). These results suggest that the drugs inhibited osteoclast differentiation by interfering with RANKL singling pathways upstream of NFATc1 induction.

We next examined the effects of MTX, Buc, and SASP on osteoclast differentiation in the coculture system with osteoblasts. In the coculture system, $VitD_3$ and PGE_2 are used to induce RANKL expression on the osteoblasts, and this system is useful in analyzing the effects of drugs on mesenchymal cells such as osteoblasts and synovial fibroblasts in addition to osteoclast precursor cells.[22,35] The same concentrations of MTX, Buc and SASP as in Fig. 1c were added to the coculture system (Fig. 2a). At these concentrations, there were no toxic effects of these drugs on the osteoblasts (data not shown). MTX and SASP exhibited greater inhibitory effects on the formation of $TRAP^+$ MNCs than in the RANLK/M-CSF system (Fig. 2b), suggesting that MTX and SASP exert anti-osteoclastogenic effects additionally through their effects on mesenchymal cells. In contrast, the inhibitory effects of Buc on the formation of $TRAP^+$ MNCs in the coculture system is similar to those in the RANKL/M-CSF system (Fig. 2b), suggesting that Buc mainly acts on osteoclast precursor cells to inhibit osteoclastogenesis. The photographs of $TRAP^+$ MNCs cultured in the presence of these drugs indicate that the size of the $TRAP^+$ MNCs was smaller than the non-treated cells and the number of nuclei per multinucleated cell was decreased in cells treated with the three drugs (Fig. 2c).

Consistent with the additional inhibitory effects of SASP and MTX on the coculture system in comparison with the RANKL/M-CSF system, it has been reported that both SASP and MTX have an inhibitory effect on RANKL expression in synovial cells.[35] However, it remains unknown how Buc acts on the expression of RANKL on the osteoclastogenesis-supporting cells. Therefore, we evaluated mRNA expression of RANKL in the osteoblasts stimulated with $VitD_3$ and PGE_2 in the presence of Buc in comparison with SASP. As expected, SASP strongly inhib-

ited the mRNA expression of RANKL on osteoblasts, but Buc had only minimal effects on RANKL expression (Fig. 2d). This result further supports the notion that Buc mainly targets osteoclast precursor cells in terms of its inhibitory effect on osteoclastogenesis. Thus, antirheumatic drugs affect osteoclastogenesis through different target cells.

To gain mechanistic insight into the efficacy obtained with the combined use of antirheumatic drugs in the treatment of RA, we evaluated the effects of a combination of MTX, Buc and SASP on osteoclast differentiation in the RANKL/M-CSF system. The addition of a low dose of MTX alone had a limited suppressive effect on osteoclastogenesis, but a combined addition with Buc or SASP increased the inhibitory effects (Fig. 3a, b). The combined use of all three drugs had a marked inhibitory effect on osteoclastogenesis, even though the addition of individual drugs at the same concentration had only a slight effect (Fig. 3a, b).

In addition, we quantitated the protein level of NFATc1 in the RANKL-stimulated BMMs after immunostaining, and this revealed that RANKL-induced NFATc1 expression was significantly inhibited by treatment with a combination of the three drugs (Fig. 3c), although treatment with individual drugs at the same concentration had only a small effect on NFATc1 expression (Fig. 1e). Interestingly, the photograph of $TRAP^+$ MNCs showed that the multinucleation was severely impaired in the cells treated with a combination of the three drugs (Fig. 3b). Therefore, we investigated the number of $TRAP^+$ MNCs containing more than 20 nuclei. We found that the number of such large osteoclasts was dramatically suppressed by the combined addition of the three antirheumatic drugs (Fig. 3d). It is worth noting that even a very low dose of MTX (0.1 nM) in combination with Buc and SASP exerted a much more suppressive effect than an addition of the same concentration of MTX alone (Fig. 3d). These results suggest that the combination with other antirheumatic drugs contributes to the enhancement of the inhibitory effect of MTX in terms of differentiation into large osteoclasts with numerous nuclei.

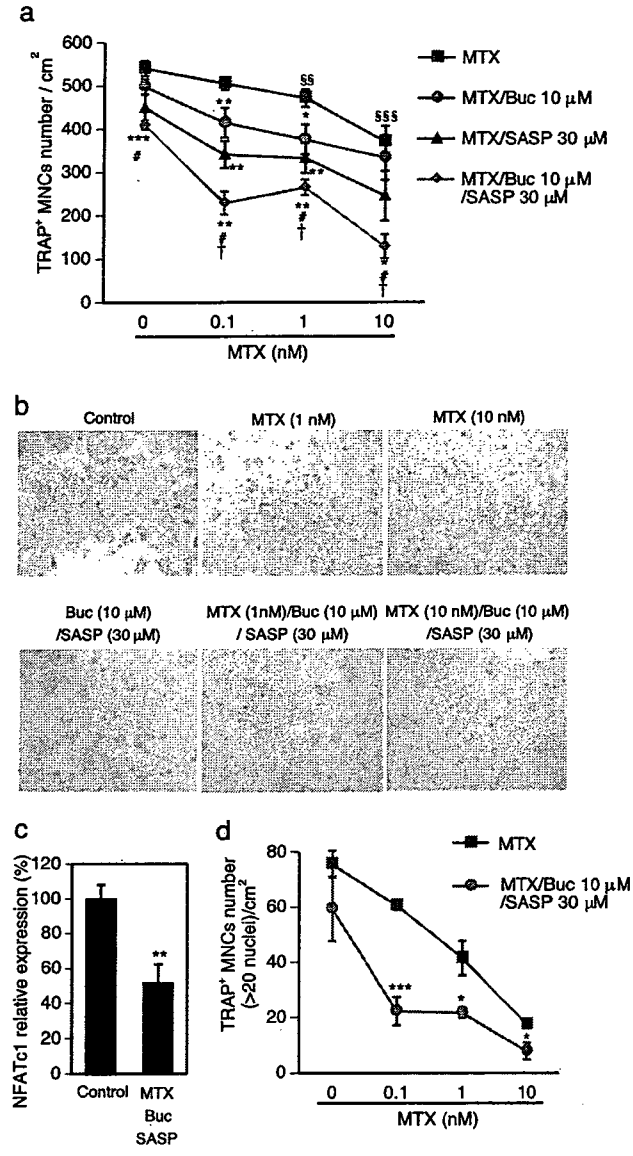

Fig. 3. Effects of methotrexate (*MTX*) alone or with the combined addition of bucillamine (*Buc*) and/or salazosulphapyridine (*SASP*) on osteoclastogenesis in the RANKL/M-CSF system. **a** Effects of MTX alone or MTX plus Buc (10μM) and/or SASP (30μM) on RANKL-induced osteoclastogenesis. $^{§§}P < 0.05$, $^{§§§}P < 0.001$ versus untreated BMMs. $*P < 0.05$, $**P < 0.01$, $***P < 0.001$ versus MTX-treated BMMs. $\#P < 0.01$ versus MTX/Buc-treated BMMs. $^{\dagger}P < 0.05$ versus MTX/SASP-treated BMMs. **b** Microscopic photographs of RANKL-induced osteoclastogenesis in cells treated with MTX alone or MTX plus Buc and/or SASP (TRAP staining). **c** Expression of *NFATc1* protein in RANKL-stimulated BMMs treated with a combination of MTX (10nM), Buc (10μM) and SASP (30μM). **d** Effect of the combined addition of MTX, Buc, and SASP on the formation of *$TRAP^+$ MNCs* containing more than 20 nuclei. Statistical analysis was performed in comparison with MTX-treated cells

Discussion

It has long been a challenging question as to how abnormalities of the immune system induce bone damage in RA.[1,2,37] Although the observation of giant cells at the bone destruction site dates back to about two decades ago,[38] osteoclasts have not been placed at the center of the pathogenesis of RA. After RANKL was cloned and the high RANKL expression in the synovium was brought to light, the importance of bone-resorbing osteoclasts gained general acceptance.[3,12] RANKL is abundantly expressed by RA synovial fibroblasts, possibly due to stimulation with proinflammatory cytokines.[18,22,39] In addition, RANKL is expressed in activated T cells,[27] although the effects of T cells on osteoclastogenesis are counterbalanced by negative factors such as IFN-γ.[33]

How is T cell activation linked to the enhanced expression of RANKL in RA? A recent study in our laboratory revealed that interleukin (IL)-17-producing helper T (Th) 17 cells play a distinct role in the pathogenesis of autoimmune arthritis and promote osteoclastogenesis, mostly through the production of IL-17.[37] As summarized in Fig. 4,

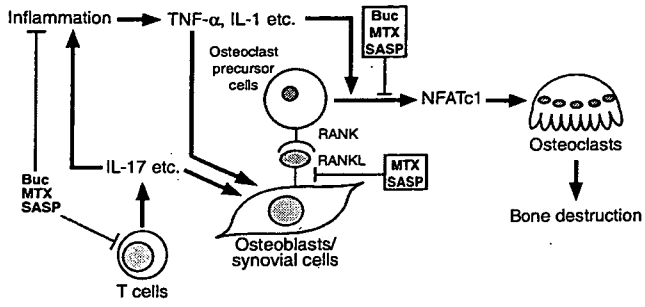

Fig. 4. How antirheumatic drugs, including methotrexate (*MTX*), bucillamine (*Buc*) and salazosulphapyridine (*SASP*) inhibit the pathways promoting bone destruction in rheumatoid arthritis (RA). Among the T-cell-derived mediators of inflammation, interleukin *(IL)-17* has emerged as one of the most important factors in the pathogenesis of RA. IL-17 not only induces *RANKL* on osteoblasts/synovial fibroblasts of mesenchymal origin, but also activates local inflammation, leading to the upregulation of inflammatory cytokines such as TNF-α and IL-1. These cytokines also induce RANKL on mesenchymal cells and additionally act directly on the osteoclast precursor cells to greatly enhance the RANKL activity. RANKL activates the differentiation of osteoclasts by inducing the expression of *NFATc1*, the master transcription factor for osteoclastogenesis. In this study, we showed that MTX, Buc and SASP suppress RANKL-induced NFATc1 expression, and that MTX and SASP inhibit RANKL expression on mesenchymal cells (shown in *boxes*). It has been previously reported that these three drugs exert inhibitory effects on the activation of T cells and inflammatory responses of synovial cells (shown in the *left lower section*)

IL-17 induces RANKL on mesenchymal cells (synovial fibroblasts/osteoblasts) and also stimulates local inflammation by inducing proinflammatory cytokines such as IL-1 and TNF-α, which in turn induces RANKL expression on mesenchymal cells.[3,40] RANKL then acts on osteoclast precursor cells of monocyte/macrophage lineage and stimulates osteoclast differentiation via the induction of NFATc1.[17,36]

This study demonstrates the mechanisms underlying the bone-protective effects of antirheumatic drugs (summarized in Fig. 4): MTX, Buc, and SASP had a suppressive effect on osteoclast differentiation by acting on osteoclast precursor cells and inhibiting RANKL-mediated expression of NFATc1 on the one hand. On the other hand, MTX and SASP had inhibitory effects on the RANKL expression in mesenchymal cells. It has been reported that MTX, Buc, and SASP inhibit the activation of T cells and inflammatory responses of synovial cells (which is also indicated in Fig. 4).[29,41–43] This may explain the anti-inflammatory effects of these drugs, but does not provide insight into how these drugs are related to the regulation of bone cells, which question we addressed experimentally in this study.

In keeping with the observation that the administration of these drugs individually has only limited clinical efficacy against bone destruction,[3,44] they have only a small inhibitory effect on osteoclast differentiation. However, such in vitro inhibitory effects is enhanced if the drugs are administered in combination. This is consistent with the efficacy of combined DMARDs therapy in comparison with the treatment with a single DMARD.[6,7,31] It was recently reported that the combination of MTX and Buc has more beneficial effects than MTX alone in treating RA patients.[45] It is likely that a combination of antirheumatic drugs that inhibit osteoclastogenesis through different mechanisms will be helpful in ameliorating or preventing bone destruction in RA.

There are a number of drugs available for the treatment for RA, but most of them were developed to modulate immune reactions.[1,5] Therefore, antirheumatic drugs, effective in treating pain and inflammation, do not always have bone-protective effects: patients still fairly frequently have to undergo joint replacement surgery because of the progressive bone damage that develops despite treatment with antirheumatic drugs.[3,46] This study provides a beneficial method to screen antirheumatic drugs for their efficacy against bone destruction. Despite the remarkable impact of anti-cytokine therapies on the treatment of RA,[47] it scarcely needs saying that antirheumatic drugs will continue to occupy a substantially important position in the foreseeable future.[5,8] The mechanism of action of antirheumatic drugs in the context of bone destruction has been poorly understood, but the identification of an effective set of existing antirheumatic drugs by means of in vitro osteoclast culture systems is a promising strategy for improving the future treatment of RA.

Acknowledgments We thank Santen Pharmaceutical Co., Ltd. and H. Aono for providing reagents and technical advice. We also thank K. Sato, H.J. Gober, T. Koga, and I. Takayanagi for fruitful discussion and assistance. This work was supported in part by Grant-in-Aid for Creative Scientific Research from the Japan Society for the Promotion of Science (JSPS), SORST program of JST, grants for Genome Network Project from Ministry of Education, Culture, Sports, Science, and Technology of Japan (MEXT), grants for the 21st Century COE program from MEXT, Grants-in-Aid for Scientific Research from MEXT, Health Sciences Research Grants from the Ministry of Health, Labour and Welfare of Japan, and grants from the Naito Foundation, Suzuken Memorial Foundation, Uehara Memorial Foundation, Kato Memorial Bioscience Foundation, Cell Science Research Foundation, the Ichiro Kanehara Foundation, Inamori Foundation and the Nakatomi Foundation. The authors declare no competing financial interests.

References

1. Takayanagi H. Osteoimmunological insight into bone damage in rheumatoid arthritis. Mod Rheumatol 2005;15:225–31.
2. Firestein GS. Evolving concepts of rheumatoid arthritis. Nature 2003;423:356–61.
3. Sato K, Takayanagi H. Osteoclasts, rheumatoid arthritis, and osteoimmunology. Curr Opin Rheumatol 2006;18:419–26.
4. Takayanagi H. Inflammatory bone destruction and osteoimmunology. J Periodontal Res 2005;40:287–93.
5. Smolen JS, Steiner G. Therapeutic strategies for rheumatoid arthritis. Nat Rev Drug Discov 2003;2:473–88.
6. Le Loet X, Berthelot JM, Cantagrel A, Combe B, De Bandt M, Fautrel B, et al. Clinical practice decision tree for the choice of the first disease modifying antirheumatic drug for very early rheumatoid arthritis: a 2004 proposal of the French Society of Rheumatology. Ann Rheum Dis 2006;65:45–50.
7. Dougados M, Combe B, Cantagrel A, Goupille P, Olive P, Schattenkirchner M, et al. Combination therapy in early rheumatoid arthritis: a randomised, controlled, double blind 52 week clinical trial of sulphasalazine and methotrexate compared with the single components. Ann Rheum Dis 1999;58:220–5.
8. Klareskog L, van der Heijde D, de Jager JP, Gough A, Kalden J, Malaise M, et al. Therapeutic effect of the combination of etanercept and methotrexate compared with each treatment alone in

patients with rheumatoid arthritis: double-blind randomised controlled trial. Lancet 2004;363:675–81.
9. Teitelbaum SL, Ross FP. Genetic regulation of osteoclast development and function. Nat Rev Genet 2003;4(8):638–49.
10. Boyle WJ, Simonet WS, Lacey DL. Osteoclast differentiation and activation. Nature 2003;423:337–42.
11. Suda T, Takahashi N, Udagawa N, Jimi E, Gillespie MT, Martin TJ. Modulation of osteoclast differentiation and function by the new members of the tumor necrosis factor receptor and ligand families. Endocr Rev 1999;20:345–57.
12. Theill LE, Boyle WJ, Penninger JM. RANK-L and RANK: T cells, bone loss, and mammalian evolution. Annu Rev Immunol 2002;20: 795–823.
13. Takayanagi H. Mechanistic insight into osteoclast differentiation in osteoimmunology. J Mol Med 2005;83:170–9.
14. Koga T, Inui M, Inoue K, Kim S, Suematsu A, Kobayashi E, et al. Costimulatory signals mediated by the ITAM motif cooperate with RANKL for bone homeostasis. Nature 2004;428:758–63.
15. Ross FP, Teitelbaum SL. Alphavbeta3 and macrophage colony-stimulating factor: partners in osteoclast biology. Immunol Rev 2005;208:88–105.
16. Walsh MC, Kim N, Kadono Y, Rho J, Lee SY, Lorenzo J, et al. Osteoimmunology: interplay between the immune system and bone metabolism. Annu Rev Immunol 2006;24:33–63.
17. Takayanagi H, Kim S, Koga T, Nishina H, Isshiki M, Yoshida H, et al. Induction and activation of the transcription factor NFATc1 (NFAT2) integrate RANKL signaling in terminal differentiation of osteoclasts. Dev Cell 2002;3:889–901.
18. Yasuda H, Shima N, Nakagawa N, Yamaguchi K, Kinosaki M, Mochizuki S, et al. Osteoclast differentiation factor is a ligand for osteoprotegerin/osteoclastogenesis-inhibitory factor and is identical to TRANCE/RANKL. Proc Natl Acad Sci USA 1998;95: 3597–602.
19. Takahashi N, Akatsu T, Udagawa N, Sasaki T, Yamaguchi A, Moseley JM, et al. Osteoblastic cells are involved in osteoclast formation. Endocrinology 1988;123:2600–2.
20. Urushibara M, Takayanagi H, Koga T, Kim S, Isobe M, Morishita Y, et al. The antirheumatic drug leflunomide inhibits osteoclastogenesis by interfering with receptor activator of NF-κB ligand-stimulated induction of nuclear factor of activated T cells c1. Arthritis Rheum 2004;50:794–804.
21. Gravallese EM, Goldring SR. Cellular mechanisms and the role of cytokines in bone erosions in rheumatoid arthritis. Arthritis Rheum 2000;43:2143–51.
22. Takayanagi H, Iizuka H, Juji T, Nakagawa T, Yamamoto A, Miyazaki T, et al. Involvement of receptor activator of nuclear factor kB ligand/osteoclast differentiation factor in osteoclastogenesis from synoviocytes in rheumatoid arthritis. Arthritis Rheum 2000;43:259–69.
23. Takayanagi H, Oda H, Yamamoto S, Kawaguchi H, Tanaka S, Nishikawa T, et al. A new mechanism of bone destruction in rheumatoid arthritis: synovial fibroblasts induce osteoclastogenesis. Biochem Biophys Res Commun 1997;240:279–86.
24. Pettit AR, Ji H, von Stechow D, Muller R, Goldring SR, Choi Y, et al. TRANCE/RANKL knockout mice are protected from bone erosion in a serum transfer model of arthritis. Am J Pathol 2001;159:1689–99.
25. Redlich K, Hayer S, Ricci R, David JP, Tohidast-Akrad M, Kollias G, et al. Osteoclasts are essential for TNF-α-mediated joint destruction. J Clin Invest 2002;110:1419–27.
26. Takayanagi H, Juji T, Miyazaki T, Iizuka H, Takahashi T, Isshiki M, et al. Suppression of arthritic bone destruction by adenovirus-mediated csk gene transfer to synoviocytes and osteoclasts. J Clin Invest 1999;104:137–46.
27. Kong YY, Feige U, Sarosi I, Bolon B, Tafuri A, Morony S, et al. Activated T cells regulate bone loss and joint destruction in adjuvant arthritis through osteoprotegerin ligand. Nature 1999;402: 304–9.
28. Lubberts E, Joosten LA, Chabaud M, van Den Bersselaar L, Oppers B, Coenen-De Roo CJ, et al. IL-4 gene therapy for collagen arthritis suppresses synovial IL-17 and osteoprotegerin ligand and prevents bone erosion. J Clin Invest 2000;105:1697–710.
29. Ranganathan P, McLeod HL. Methotrexate pharmacogenetics: the first step toward individualized therapy in rheumatoid arthritis. Arthritis Rheum 2006;54:1366–77.
30. Sekiguchi N, Kameda H, Amano K, Takeuchi T. Efficacy and safety of bucillamine, a D-penicillamine analogue, in patients with active rheumatoid arthritis. Mod Rheumatol 2006;16:85–91.
31. Nagashima M, Shu G, Yamamoto K, Yamahatsu S, Yoshino S. The ability of disease modifying antirheumatic drugs to induce and maintain improvement in patients with rheumatoid arthritis. epidemiology of DMARDs treatment in Japan. Clin Exp Rheumatol 2005;23:27–35.
32. Tsuji F, Aono H, Okamoto M, Sasano M. Bucillamine, A unique anti-rheumatic drug. Curr Top Pharmacol [in press].
33. Takayanagi H, Ogasawara K, Hida S, Chiba T, Murata S, Sato K, et al. T-cell-mediated regulation of osteoclastogenesis by signalling cross-talk between RANKL and IFN-γ. Nature 2000;408:600–5.
34. Koga T, Matsui Y, Asagiri M, Kodama T, de Crombrugghe B, Nakashima K, et al. NFAT and Osterix cooperatively regulate bone formation. Nat Med 2005;11:880–5.
35. Lee CK, Lee EY, Chung SM, Mun SH, Yoo B, Moon HB. Effects of disease-modifying antirheumatic drugs and anti-inflammatory cytokines on human osteoclastogenesis through interaction with receptor activator of nuclear factor κB, osteoprotegerin, and receptor activator of nuclear factor κB ligand. Arthritis Rheum 2004;50:3831–43.
36. Asagiri M, Sato K, Usami T, Ochi S, Nishina H, Yoshida H, et al. Autoamplification of NFATc1 expression determines its essential role in bone homeostasis. J Exp Med 2005;202:1261–9.
37. Sato K, Suematsu A, Okamoto K, Yamaguchi A, Morishita Y, Kadono Y, et al. Th17 functions as an osteoclastogenic helper T cell subset that links T cell activation and bone destruction. J Exp Med 2006;203:2673–82.
38. Bromley M, Woolley DE. Chondroclasts and osteoclasts at subchondral sites of erosion in the rheumatoid joint. Arthritis Rheum 1984;27:968–75.
39. Schett G, Hayer S, Zwerina J, Redlich K, Smolen JS. Mechanisms of disease: the link between RANKL and arthritic bone disease. Nat Clin Pract Rheumatol 2005;1:47–54.
40. Dong C. Diversification of T-helper-cell lineages: finding the family root of IL-17-producing cells. Nat Rev Immunol 2006;6:329–33.
41. Munakata Y, Iwata S, Dobers J, Ishii T, Nori M, Tanaka H, et al. Novel in vitro effects of bucillamine: inhibitory effects on proinflammatory cytokine production and transendothelial migration of T cells. Arthritis Rheum 2000;43:1616–23.
42. Aono H, Hasunuma T, Fujisawa K, Nakajima T, Yamamoto K, Mita S, et al. Direct suppression of human synovial cell proliferation in vitro by salazosulfapyridine and bucillamine. J Rheumatol 1996;23:65–70.
43. Liptay S, Bachem M, Hacker G, Adler G, Debatin KM, Schmid RM. Inhibition of nuclear factor κB and induction of apoptosis in T-lymphocytes by sulfasalazine. Br J Pharmacol 1999;128:1361–9.
44. Breedveld FC, Emery P, Keystone E, Patel K, Furst DE, Kalden JR, et al. Infliximab in active early rheumatoid arthritis. Ann Rheum Dis 2004;63:149–55.
45. Ichikawa Y, Saito T, Yamanaka H, Akizuki M, Kondo H, Kobayashi S, et al. Therapeutic effects of the combination of methotrexate and bucillamine in early rheumatoid arthritis: a multicenter, double-blind, randomized controlled study. Mod Rheumatol 2005;15:323–8.
46. Choy EH, Panayi GS. Cytokine pathways and joint inflammation in rheumatoid arthritis. N Engl J Med 2001;344:907–16.
47. Feldmann M, Maini RN. Anti-TNFα therapy of rheumatoid arthritis: what have we learned? Annu Rev Immunol 2001;19:163–96.

0013-7227/07/$15.00/0
Printed in U.S.A.

Endocrinology 148(6):2708–2715

doi: 10.1210/en.2007-0215

Overexpression of γ-Glutamyltransferase in Transgenic Mice Accelerates Bone Resorption and Causes Osteoporosis

Kiyoshi Hiramatsu, Yutaro Asaba, Sunao Takeshita, Yuji Nimura, Sawako Tatsumi, Nobuyoshi Katagiri, Shumpei Niida, Toshihiro Nakajima, Sakae Tanaka, Masako Ito, Gerard Karsenty, and Kyoji Ikeda

Department of Bone and Joint Disease (K.H., Y.A., S.Tak., S.Tat., N.K., S.N., K.I.) Research Institute, National Center for Geriatrics and Gerontology (NCGG), Obu, Aichi 474-8522, Japan; Department of Surgery (K.H., Y.A., Y.N.), Nagoya University Graduate School of Medicine, Nagoya 466-8550, Japan; National Institute of Biomedical Innovation (S.Tat.), Osaka 567-0085, Japan; Department of Genome Science (T.N.), Institute of Medical Science, St. Marianna University of Medicine, Kanagawa 216-8512, Japan; Department of Orthopedic Surgery (S.Tan.), University of Tokyo School of Medicine, Tokyo 113-8655, Japan; Department of Radiology (M.I.), Nagasaki University School of Medicine, Nagasaki 852-8501, Japan; and Department of Genetics and Development (G.K.), Columbia University, New York, New York 10032

We previously identified γ-glutamyltransferase (GGT) by expression cloning as a factor inducing osteoclast formation *in vitro*. To examine its pathogenic role *in vivo*, we generated transgenic mice that overexpressed GGT in a tissue-specific manner utilizing the Cre-loxP recombination system. Systemic as well as local production of GGT accelerated osteoclast development and bone resorption *in vivo* by increasing the sensitivity of bone marrow macrophages to receptor activator of nuclear factor-κB ligand, an essential cytokine for osteoclastogenesis. Mutated GGT devoid of enzyme activity was as potent as the wild-type molecule in inducing osteoclast formation, suggesting that GGT acts not as an enzyme but as a cytokine. Recombinant GGT protein increased receptor activator of nuclear factor-κB ligand expression in marrow stromal cells and also stimulated osteoclastogenesis from bone marrow macrophages at lower concentrations. Thus, GGT is implicated as being involved in diseases characterized by accelerated osteoclast development and bone destruction and provides a new target for therapeutic intervention. (*Endocrinology* 148: 2708–2715, 2007)

AGE-RELATED DISORDERS of the skeletal system are a major health problem worldwide (1, 2), and osteoclastic bone resorption plays a central role in the pathogenesis of bone and joint diseases, such as osteoporosis and rheumatoid arthritis (3). Osteoclasts are multinucleate, giant cells derived from hematopoietic progenitor cells of monocyte-macrophage lineage and are the only cell type that resorbs bone to maintain skeletal integrity and calcium homeostasis (4). The dysregulated generation of osteoclasts with resultant elevation of bone resorption that takes place after menopause and with aging or as an immune/inflammatory response leads to osteoporotic fractures and the joint destruction associated with rheumatoid arthritis (5). Genetic studies on human patients as well as mutant mice have disclosed critical molecules involved in osteoclast development, including cytokines, intracellular signaling molecules, and nuclear transcription factors (3, 4). Among these, the osteoclastogenic cytokines have received special attention, because they represent novel targets for the development of both diagnostic tools and antiresorptive drugs (6). For example, receptor activator of nuclear factor-κB ligand (RANKL), belonging to the TNF family (6), was identified as an essential cytokine for osteoclastogenesis, and mice deficient in RANKL were found to lack osteoclasts completely and to exhibit severe osteopetrosis (7).

In an attempt to identify new cytokines that stimulate osteoclast differentiation, we employed an expression cloning strategy, where cRNA from T lymphoma cells known to possess high bone resorption activity was injected into *Xenopus* oocytes (8). By assaying the conditioned medium for osteoclastogenic activity in murine marrow cultures, we identified γ-glutamyltransferase (GGT) as such a stimulator (9). GGT is an ectopeptidase that catalyzes the transfer of a γ-glutamyl moiety to an acceptor and plays a critical role in glutathione degradation and cysteine metabolism (10, 11). Mice deficient in GGT exhibit growth retardation, cataracts, and severe osteoporosis and die at 10–18 wk of age (12, 13). We have found that purified GGT from rat kidney is capable of inducing osteoclast formation in bone marrow cultures *in vitro* (9), which raises the possibility that its excess may also be involved in the bone and joint pathology characterized by enhanced osteoclastic bone resorption. The transgenic mice obtained by the Cre-loxP recombination system in the present study produce GGT systemically as well as locally, demonstrating that GGT indeed contributes to bone destruction, independently of its enzymatic activity, by acting as a local cytokine.

First Published Online March 15, 2007

Abbreviations: CT, Computed tomography; DPD, deoxypyridinoline; eGFP, enhanced green fluorescent protein; KO, knockout; M-CSF, macrophage colony-stimulating factor; pmtGGT, point-mutated GGT; RANKL, receptor activator of nuclear factor-κB ligand; TRAP, tartrate-resistant acid phosphatase.

Endocrinology **is published monthly by The Endocrine Society (http://www.endo-society.org), the foremost professional society serving the endocrine community.**

Materials and Methods

Reagents

Mouse macrophage colony-stimulating factor (M-CSF) and soluble RANKL were purchased from R&D Systems (Minneapolis, MN). Rabbit polyclonal anti-GGT antibody was a generous gift from Dr. N. Taniguchi (Osaka University, Osaka, Japan).

Generation of transgenic mice and animal experiments

A transgenic cassette (floxed eGFP-GGT) carrying a CAG promoter and an enhanced green fluorescent protein (eGFP) flanked by loxP sites fused to mouse GGT cDNA with a polyadenylation signal was constructed. Mouse GGT cDNA was synthesized from RNA extracted from the kidney of C57BL/6 mouse, and Kozac sequences and *Mfe*I restriction sites were added by using a primer set (5′-CCGCAATTGCCACCATGAAGAATCGGTTTCTGGTGC-3′ and 5′-CCGCAATTGTCAGTAGCCAGCAGGTTCCCCGCC-3′). This GGT cDNA fragment was inserted into *Eco*RI-digested pCXP/loxGFP, which contained CAG promoter and eGFP (14). The transgenic construct was excised with *Sal*I and *Hind*III endonucleases and purified by using standard techniques.

Founder floxed eGFP-GGT mice were generated by microinjection of the DNA into fertilized eggs of C57BL/6 mice. Integration of the transgene was identified by green fluorescence and confirmed by Southern and PCR analyses of genomic DNA extracted from the tail, by using the following primers: 5′-GGTGTTCTGCCGCCAAGGGAAGG-3′ and 5′-GAGACACATCGACAAACTTTGGG-3′ for GGT and 5′-TGAACCGCATCGAGCTGAAGGG-3′ and 5′-TCCAGCAGGACCATGTGATCGC-3′ for eGFP. Floxed eGFP-GGT mice were crossed with CAG-Cre (15), RANKL knockout (KO) (7), and Col I-Cre (16) mice, to generate GGT-Tg, GGT-Tg/RANKL KO, and Col I-GGT mice, respectively.

Mice were raised under standard laboratory conditions at 24 ± 2 C and 50–60% humidity and allowed free access to tap water and commercial standard rodent chow (CE-2) containing 1.20% calcium, 1.08% phosphate, and 240 IU/100 g vitamin D_3 (Clea Japan Inc., Tokyo, Japan). Both male and female mice were analyzed at the age of 9 wk. Urine was collected during the final 24 h, and blood samples were centrifuged to obtain the serum.

All experiments were performed in accordance with NCGG's ethical guidelines for animal care, and the experimental protocols were approved by the animal care committee.

Bone and histological analyses

For bone analysis, right tibiae were dissected and stored in 70% ethanol for microcomputed tomography (micro-CT) scanning. Left tibiae were fixed in 4% paraformaldehyde, and bone histomorphometry was performed on un-decalcified sections, with tetracycline and calcein double labeling, as described previously (17). Histomorphometric parameters were measured at Niigata Bone Science Institute (Niigata, Japan).

Micro-CT scanning was performed on proximal tibiae by using a μCT-40 (SCANCO Medical AZ, Bassersdorf, Switzerland) with a resolution of 12 μm, and microstructure parameters were calculated three-dimensionally as described previously (18).

Biochemistry

Serum and urinary calcium, phosphate, creatinine, and GGT concentrations were determined by an autoanalyzer (Hitachi 7170, Tokyo, Japan). Urinary deoxypyridinoline (DPD) was measured with a Pyrilinks-D assay kit (Metra Biosystems Inc., Santa Clara, CA). Tissue GGT activity was determined using a γ-GTP C-TestWako kit (Wako Pure Chemical Industries Ltd., Osaka, Japan) with L-γ-glutamyl-*p*-*N*-ethyl-*N*-hydroxyethylaminoanilide as the substrate and glycylglycine as the acceptor, as described earlier (19).

Cell cultures and osteoclastogenesis assay in vitro

HEK293 cells were transfected with the transgenic cassette (floxed eGFP-GGT) described above, with or without Cre recombinase, to confirm that the DNA construct functioned as designed.

Bone marrow cells were isolated from the tibiae and femurs of 6- to 9-wk-old male C57BL/6J mice (SLC, Shizuoka, Japan), and osteoclastogenesis assays were performed as described previously (20). In brief, bone marrow cells were plated in culture dishes containing α-MEM, 10% heat-inactivated fetal bovine serum, antibiotics, and 1/10 volume of CMG14–12 culture supernatant (as a source of M-CSF). After 3 d culture, adherent cells were used as osteoclast precursor cells. Cells were then cultured with M-CSF (50 ng/ml) and soluble RANKL (50 ng/ml) for 4 d, fixed in 4% paraformaldehyde, and stained for tartrate-resistant acid phosphotase (TRAP). In some experiments, recombinant GGT was added at various concentrations to the culture. The number of multinucleate (at least three nuclei), TRAP-positive cells was counted as osteoclasts. Pit assay was performed on dentin slices as previously described (20), and analysis of pit area was performed on a Macintosh computer using the public domain NIH Image program (developed at the United States National Institutes of Health and available on the internet at http://rsb.info.nih.gov/nih-image/).

Expression and purification of recombinant GGT

Recombinant GGT protein was generated using the baculovirus/insect cell system as described previously (21). In brief, human GGT cDNA in a pKBLgp64 vector (Oriental Yeast Co., Ltd, Tokyo, Japan) was cotranfected with DHBac10 (Invitrogen, San Diego, CA) using Cellfectin (Invitrogen) into Sf9 cells, which were then infected by the recombinant viruses. Cells were harvested, and the protein was extracted with 10 mM sodium phosphate buffer (pH 6.5)/1% Triton X-100 and further solubilized by protease treatment. The solubilized protein was purified through a hydroxylapatite column and isoelectric chromatography using PBE 94 (Pharmacia, Piscataway, NJ) and Polybuffer 74. The eluate was passed through a Sephacryl S-200 HR (Pharmacia) gel filtration column to remove the Polybuffer.

Site-directed mutagenesis of GGT and retroviral expression

Serine residues at 451 and 452 of mouse GGT were replaced by alanine by site-directed mutagenesis using the QuikChange Multi Site-Directed Mutagenesis Kit (Stratagene, La Jolla, CA) according to the manufacturer's instructions. In brief, oligonucleotide primers containing mutations (5′-GGTAAGCAGCCTCTTGCAGCCATGTGTCCCTCAATC-3′ and 5′-GATTGAGGGACACATGGCTGCAAGAGGCTGCTTACC-3′) were annealed to template DNA, and the mutant strand was synthesized and amplified by using *PfuTurbo* DNA polymerase (at 95 C for 30 sec, 55 C for 1 min, and 68 C for 5 min for 18 cycles). After the reaction products were treated with *Dpn*I endonuclease, the mutated DNA was transformed into XL 10-Gold ultracompetent cells. Plasmid DNA was prepared from the transformants, and the mutated sequences were confirmed.

Retroviral vectors encoding wild-type and mutated GGT were used to transfect the retrovirus packaging cells, Plat-E (a gift from Dr. T. Kitamura, University of Tokyo) or GP2-293 (Clontech Laboratories, Inc., Palo Alto, CA). Osteoclast precursor cells were exposed to the retrovirus in the presence of polybrene (4 μg/ml) and M-CSF for 1 d and were subsequently treated with RANKL and M-CSF for 4 d in the presence of puromycin (1.6 μg/ml). Osteoclast differentiation was evaluated as described above. The retrovirus was also infected to primary osteoblasts isolated from newborn mouse calvaria, and alkaline phosphatase activity was assessed.

Northern and RT-PCR analyses

Total RNA was isolated with TRIzol Reagent (Invitrogen), and equal amounts (10 μg/lane) were fractionated on a 1.5% agarose gel. The specific mRNAs were detected by hybridization of Hybond N+ nylon membranes (Amersham Biosciences, Inc., Piscataway, NJ) with ^{32}P-labeled cDNA probes. For quantitative RT-PCR, total RNA (1 μg) was reverse transcribed by using Superscript III (Invitrogen); and samples were analyzed using a Light Cycler system (Roche Diagnostics, Basel, Switzerland). The primers included 5′-CCCGTGCTGATTCTCATCTT-3′ and 5′-GCATAGGCAAACCGAAAGG-3′ for GGT, 5′-TGGAAGGCTCATGGTTGGAT-3′ and 5′-CATTGATGGTGAGGTGTGCAA-3′ for RANKL, 5′-GCTGGCTACCACTGGAACTC-3′ and 5′-TGTGCACACCGTATCCTTGT-3′ for RANK, 5′-ACCTGTTCGTGAAACACACCA-3′ and 5′-CTCAGACTGTCCTTCAAGGC-3′ for *c-fos*, 5′-

GCAAAGATGGAAACGACCTTCTAC-3′,5′-GGCCAGGTTCAAGGTCA T GCTCT-3′ for *c-jun*, 5′-TGCAAGCGCTCACCGTCTAC-3′, 5′-ACCGACA-GATACTGCTCGCAAA-3′ for NFATc1, and 5′-TGCTGCCATTGTT-GATATGG-3′ and 5′-TCCACAGCTTTGATGACACC-3′ for EF-1α. The amount of target mRNA was corrected by that of EF-1α mRNA.

Western blot analysis

Cells were lysed in the buffer containing 20 mM Tris-HCl (pH 7.5), 150 mM NaCl, 1 mM EDTA, 1 mM EGTA, 1% Triton X-100, 2.5 mM sodium pyrophosphate, 1 mM β-glycerophosphate, 1 mM Na_3VP_4, 1 mM NaF, and 1× protease inhibitor mixture. Cell lysates were boiled in the presence of SDS sample buffer [0.5 M Tris-HCl (pH 6.8), 10% glycerol, and 0.05% (wt/vol) bromophenol blue) for 5 min and subjected to electrophoresis on 10% SDS-PAGE. Proteins were transferred to Hybond-C extra nitrocellulose membranes from Amersham using a semidry blotter and incubated in blocking solution (5% nonfat dry milk in Tris-buffered saline containing 0.1% Tween 20) for 1 h to reduce nonspecific binding. Membranes were then exposed to anti-GGT antibody overnight at 4 C, washed three times, and incubated with goat antirabbit IgG horseradish peroxidase-conjugated antibody for 1 h. Membranes were washed extensively, and enhanced chemiluminescence detection assay was performed according to the manufacturer's instructions.

Statistical analysis

Data are expressed as the mean ± SD. Statistical analysis was performed by Student's *t* test. Values were considered statistically significant at $P < 0.05$.

Results

Generation of GGT transgenic mouse

To test whether GGT could induce osteoclast formation and stimulate bone resorption *in vivo*, we used the Cre-loxP recombination system to generate transgenic mice that produced GGT systemically or locally. As schematically illustrated in Fig. 1A, we constructed a transgenic cassette that carries floxed eGFP fused to mouse GGT cDNA with a polyadenylation signal, under the control of the chicken β-actin (CAG) promoter driving ubiquitous gene expression. When HEK293 cells were transfected with this DNA construct, green fluorescence was observed (Fig. 1B) with little GGT activity in conditioned medium or cellular extracts (Fig. 1C). Upon the introduction of Cre recombinase, GGT activity as well as its mRNA was markedly induced (Fig. 1C), whereas the green fluorescence gradually weakened (Fig. 1B), indicating that the DNA cassette functioned as designed.

Nine transgenic founders were produced using the standard pronuclear injection protocol. Floxed eGFP-GGT mice were identified by their green color (Fig. 1D), and their genotype was confirmed by the presence of the GGT transgene in genomic DNA extracted from their tails (Fig. 1E) and by Southern hybridization (data not shown). Floxed eGFP-GGT male mice were then mated to female CAG-Cre transgenic mice to generate transgenic lines that produced GGT systemically. Of the four independent transgenic founders (GGT-Tg lines) obtained, two (A and B) were found to have lost the Cre gene and therefore were propagated for further investigation by mating to C57BL/6 wild-type females, because their progeny allowed avoidance of deleterious effects due to the presence of the Cre gene. Pups of both lines were born at the expected ratio, appeared normal, grew indistinguishably from wild-type mice, and were fertile. The two lines (A and B) displayed a very similar phenotype, and the results presented are from GGT-Tg line A.

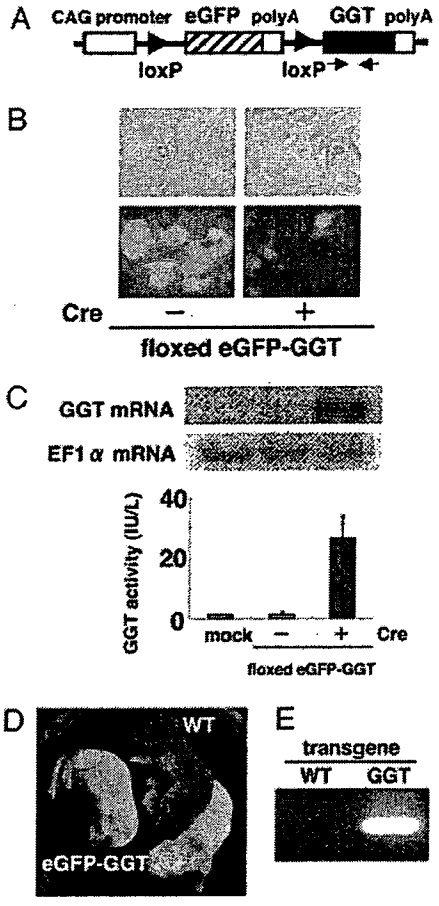

FIG. 1. Generation of floxed eGFP-GGT transgenic mice. A, Schematic representation of the transgenic construct (floxed eGFP-GGT). eGFP flanked by loxP sites fused to mouse GGT cDNA was placed under the control of a CAG promoter. *Arrows* indicate a set of primers used for confirming integration of the transgene. B and C, GFP expression in HEK293 cells transfected with the floxed eGFP-GGT construct without and with Cre recombinase transfection. *Green* fluorescence gradually decreased after introduction of the Cre gene (B), whereas the content of GGT mRNA and the activity of the enzyme in the culture supernatant were markedly induced after expression of Cre recombinase (C). D and E, Floxed GFP-GGT mice were identified by *green* color (D), and transgene expression was confirmed by PCR with the primer set shown in A (E). WT, Wild type.

Northern blot analysis of RNAs extracted from various tissues revealed that GGT mRNA was expressed predominantly in the kidney of the wild-type mouse, whereas it was found in a variety of tissues, including bone and bone marrow, in the GGT-Tg mouse (Fig. 2A). Production of actual GGT protein was also confirmed by measuring its enzymatic activity. In agreement with the mRNA tissue distribution, GGT enzymatic activity was highest in the kidney of wild-type mice, whereas the GGT-Tg mouse exhibited high enzyme activity in various tissues in addition to the kidney (Fig. 2B).

Systemic overexpression of GGT accelerates bone resorption and induces osteopenia with microstructural deterioration

GGT-Tg mice grew normally, and their body weight was indistinguishable from wild-type littermates (Fig. 2C). The data presented here are based on the analysis of 9-wk-old

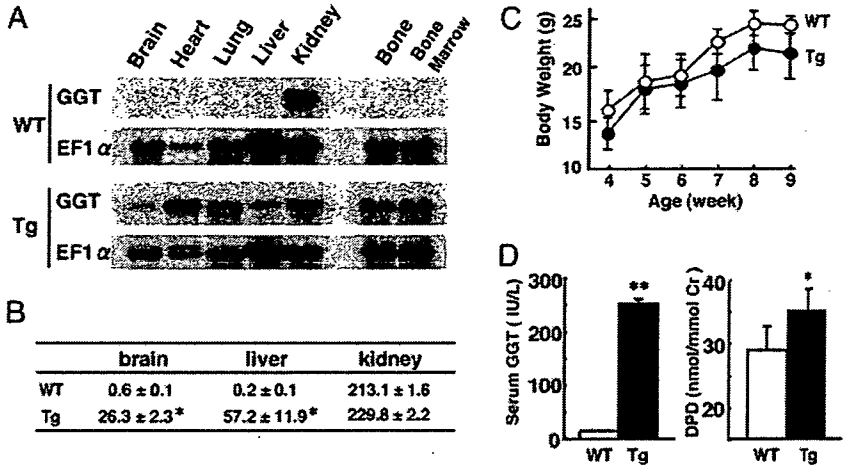

B

	brain	liver	kidney
WT	0.6 ± 0.1	0.2 ± 0.1	213.1 ± 1.6
Tg	26.3 ± 2.3*	57.2 ± 11.9*	229.8 ± 2.2

FIG. 2. Identification of GGT-Tg mice with increased GGT production. A, Tissue distribution of GGT mRNA by Northern blot analysis in various tissues from GGT-Tg mice and wild-type (WT) littermates. EF-1α mRNA was used as control for loading. B, GGT enzymatic activities (in IU/wet tissue weight) were determined in various tissues from GGT transgenic (Tg) mice and wild-type (WT) littermates. *, $P < 0.05$ (n = 3 in each group). C, Body weight of wild-type (WT) and GGT transgenic (Tg) mice. No difference was observed; n = 8 for each group. D, Serum GGT activity and urinary DPD excretion. Urinary DPD was corrected for creatinine (Cr). *, $P < 0.05$; **, $P < 0.01$ *vs.* WT (n = 8 for each group).

male mice, but a similar phenotype was observed in female mice. GGT-Tg mice exhibited a high serum concentration of GGT and significantly higher urinary excretion of DPD, a biochemical marker of bone resorption, compared with wild-type mice (Fig. 2D).

The effects of GGT overexpression on trabecular bone structure in GGT-Tg mice were analyzed by micro-CT scanning of the tibial metaphysis. As shown in Fig. 3, micro-CT images of the trabecular compartment of the proximal tibia reveal marked osteopenia with a substantial reduction in the three-dimensional-bone volume fraction (BV/TV). Microstructural analysis revealed the bone of GGT-Tg mice to be characterized by significant decreases in connectivity and trabecular thickness and number and by increases in trabecular separation and structure model index (Fig. 3B), indicating the trabeculae of GGT-Tg mice had become thinned, less connected, and converted from its normal plate-like structure to a more fragile, rod-like structure.

The effects of GGT excess on bone remodeling were further analyzed by histomorphometry at the proximal tibia. As shown in Fig. 4, as histological indices of bone resorption, the number of osteoclasts (N.Oc/BS), the bone surface covered by osteoclasts (Oc.S/BS), and the eroded surface (ES/BS), were all significantly elevated in GGT-Tg mice compared with the wild-

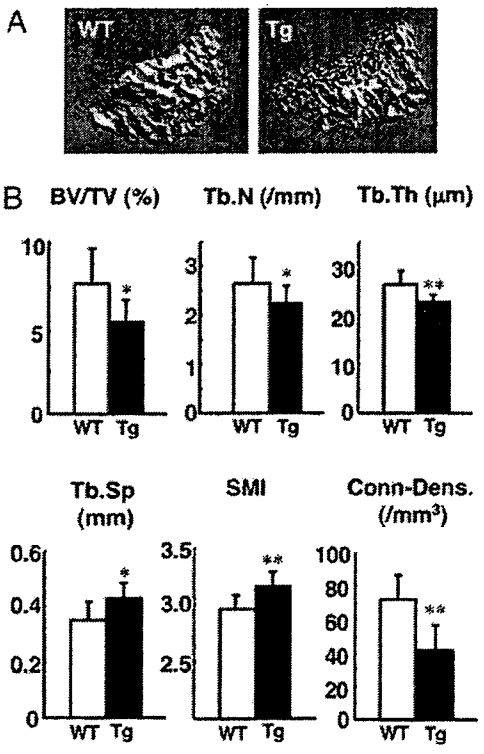

FIG. 3. GGT-Tg mice exhibit osteopenia with microstructural deterioration. A, Representative three-dimensional images obtained by micro-CT of trabecular bone at the tibiae of wild-type (WT) and of GGT transgenic (Tg) mice. B, Microstructural parameters are shown. BV/TV, Three-dimensional-bone volume fraction per tissue volume; Conn-Dens, connectivity density; Tb.N, trabecular number; Tb.Th, trabecular thickness; Tb.Sp, trabecular separation; SMI, structure model index. *, $P < 0.05$; **, $P < 0.01$ *vs.* WT (n = 7–9 for each group).

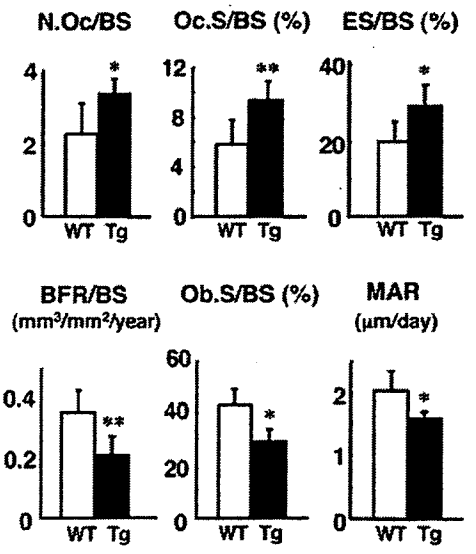

FIG. 4. GGT-Tg mice exhibit elevated bone resorption with reduced bone formation. Results of histomorphometry at the tibial metaphysis are shown. Note that GGT-Tg mice exhibit increases in indices of bone resorption (N.Oc, number of osteoclasts; Oc.S, osteoclast surface; ES, eroded surface) and decreases in parameters of bone formation (BFR, bone formation rate; Ob.S, osteoblast surface; MAR, mineral apposition rate). Data are normalized for bone surface (BS). *, $P < 0.05$; **, $P < 0.01$ *vs.* WT (n = 5 for each group).

type mice. Unexpectedly, the GGT-Tg mice revealed a lowered bone formation rate (BFR) with reduced osteoblast surface (Ob.S) and mineral apposition rate (MAR) (Fig. 4). Taken together with the elevated DPD excretion in GGT-Tg mice, these data suggest systemic overproduction of GGT accelerates bone resorption while suppressing bone formation, thus resulting in osteopenia.

Mechanism of accelerated bone resorption in GGT-Tg mouse

To gain further insight into the mechanism by which GGT stimulates osteoclast formation and bone resorption, we crossed GGT-Tg with mice lacking RANKL, an essential cytokine for osteoclastogenesis. Transgenic expression of GGT caused osteopenia on a RANKL$^{+/-}$ background (Fig. 5). Homozygous KO (RANKL$^{-/-}$) mice exhibited typical osteopetrosis with failure of tooth eruption and a complete absence of TRAP-positive osteoclasts, and GGT overexpression did not rescue these animals from the abnormal phenotypes in the absence of RANKL (Fig. 5). These results provide genetic evidence that RANKL is required for GGT to induce bone resorption.

Based on these findings, we investigated GGT modulation of the cellular response to RANKL in the presence of M-CSF. As shown in Fig. 6A, bone marrow macrophages derived from GGT-Tg mice gave rise to more and larger TRAP-positive multinucleate cells in response to RANKL, and quantitation of TRAP-positive cells with more than three nuclei indicated that the bone marrow macrophages from GGT-Tg mice generated significantly more osteoclasts than those from wild-type mice in response to RANKL. The TRAP-positive cells thus formed were functional, and those derived from GGT-Tg mice produced significantly more pits on dentin slices (Fig. 6B). These results suggest that GGT stimulates bone resorption by modulating the signaling of RANKL in osteoclast precursor cells of monocyte-macrophage lineage.

To further substantiate this concept, we extracted RNA from bone marrow cells and bone cells (cells attached to bone after flushing out the bone marrow) from both GGT-Tg and wild-type mice, and gene expression was examined by quantitative

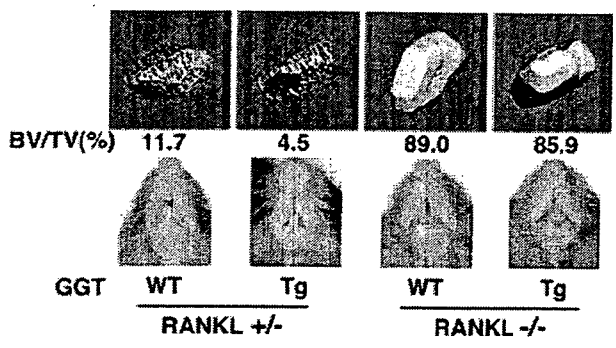

FIG. 5. RANKL is required for GGT to induce osteoclast formation. GGT-Tg mice were crossed with RANKL$^{+/-}$ mice to obtain the indicated genotypes. Representative micro-CT images of trabecular compartments of proximal tibiae are shown with the bone volume fraction (BV/TV) and the presence or absence of tooth eruption in the respective genotype. GGT-Tg induces osteopenia as a result of stimulated bone resorption on a RANKL$^{+/-}$ background, whereas GGT overexpression does not rescue RANKL$^{-/-}$ mice from their osteoclast-deficiency phenotypes, *i.e.* osteopetrosis and failure of tooth eruption.

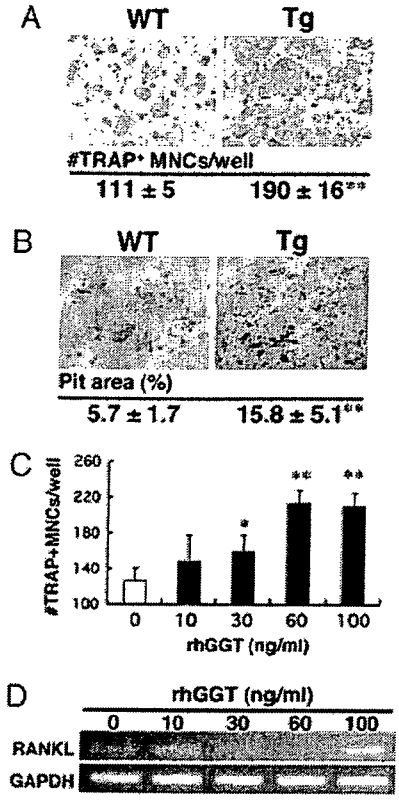

FIG. 6. GGT increases the sensitivity of bone marrow macrophages to RANKL. A, Bone marrow macrophages derived from GGT-Tg mice generated more and larger TRAP-positive osteoclasts than those from wild-type (WT) bone marrow in response to RANKL. *Ex vivo* culture was performed in the presence of M-CSF and RANKL, and the number of TRAP-positive cells with more than three nuclei was counted. B, Preosteoclasts were prepared from the bone marrow macrophages from GGT-Tg and WT mice in the presence of M-CSF and RANKL for 2 d, and then cells were incubated on dentin slices for 2 d. Resorption pits were stained with Coomassie brilliant blue. **, $P < 0.01$ *vs.* WT (n = 3 for each group). C, Recombinant human GGT (rhGGT) stimulated osteoclast formation in a dose-dependent manner. Bone marrow macrophages were cultured with M-CSF (50 ng/ml) and RANKL (25 ng/ml) in the absence or presence of the indicated concentrations of recombinant GGT protein. *, $P < 0.05$; **, $P < 0.01$ *vs.* control cultures without GGT (n = 3 for each group). D, Recombinant human GGT (rhGGT) stimulated RANKL expression. Marrow stromal cells were treated with increasing concentrations of recombinant GGT protein, and RANKL mRNA expression was analyzed by RT-PCR. GAPDH mRNA was used as an internal control.

RT-PCR. As shown in Fig. 7, expression levels of RANKL mRNA in the bone fraction and RANK mRNA in bone marrow cells did not differ significantly between the GGT-Tg and wild-type mice. In contrast, bone marrow cells from GGT-Tg mice exhibited significantly higher expression of *c-fos*, *c-jun*, and NFATc1 mRNA, which are transcription factors essential for osteoclastogenesis (22–24) (Fig. 7). The finding that critical positive regulators known to transmit the osteoclastogenic signal from the RANK receptor are up-regulated in bone marrow cells of GGT-Tg mice, although the expression of RANKL and RANK are unaltered, supports the concept that GGT acts on hematopoietic cells of monocyte-macrophage lineage to increase their sensitivity to RANKL, thereby stimulating osteoclast generation and bone resorption. Also consistent with this

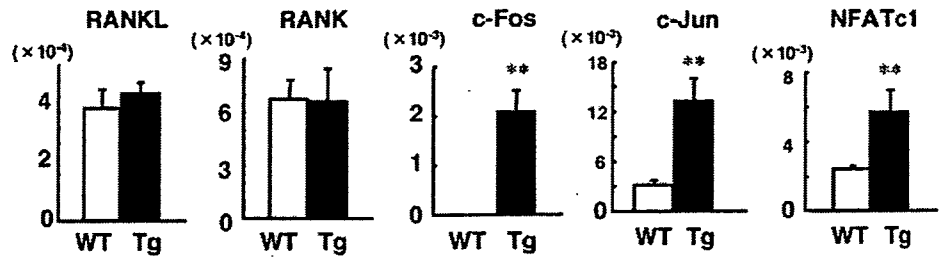

FIG. 7. Increased expression of c-Fos, c-Jun, and NFATc1 mRNA in GGT-Tg marrow cells. Expression of critical regulators of osteoclast differentiation (RANKL in bone fraction and other molecules in bone marrow fraction) in GGT-Tg *vs.* wild-type (WT) mice was examined. RNA was extracted from bone and bone marrow separately from three wild-type and three Tg mice, and mRNA levels were determined by quantitative RT-PCR. **, $P < 0.01$ *vs.* wild type.

notion are the results that recombinant GGT protein was capable of stimulating osteoclast formation from bone marrow macrophages in a dose-dependent manner, and a significant increase in osteoclastogenesis was observed at 30 ng/ml (Fig. 6C). As reported previously (9), recombinant GGT also increased the expression of RANKL mRNA in marrow stromal cells but only at the highest concentration of 100 ng/ml (Fig. 6D).

GGT-Tg mice produce GGT not only in skeletal tissue but also in various other tissues and exhibit elevated levels of circulating GGT (Fig. 2, A and D). To rule out the possibility that bone resorption was stimulated as a secondary effect of systemic overexpression of GGT and to obtain evidence that GGT acts locally in bone, we next generated transgenic lines that produce GGT only in bone tissue. Taking advantage of the original design of our floxed eGFP-GGT construction (Fig. 1A), which enables tissue-specific expression of GGT, we crossed floxed eGFP-GGT mice with Col I-Cre mice, which express Cre recombinase under the control of the 2.3-kb type I collagen promoter and have been shown to target transgenic expression specifically in osteoblasts (16), to generate Col I-GGT mice. The serum GGT concentration of Col I-GGT mice was not increased (<2 IU/liter), compared with the floxed eGFP-GGT mice used as a control, indicating that Col I-GGT mice are not characterized by systemic overproduction of GGT. TRAP staining of tibial sections revealed that significantly more TRAP-positive multinucleate osteoclasts were induced in the skeletal tissue of Col I-GGT mice than floxed eGFP-GGT mice (Fig. 8A). These results suggest that systemic elevation of GGT is not a prerequisite for its osteoclastogenic action and are consistent with the concept that GGT acts locally on bone in stimulating osteoclast formation.

To determine whether the enzymatic activity is required for the bone-resorbing activity, we introduced mutations in two consecutive serine residues at 451 and 452, which are known to be critical for the catalytic activity, by substituting them with alanine (S451A/S452A double mutant). When the point-mutated GGT (pmtGGT) was expressed in HEK293 cells at the same level as the wild-type molecule, the enzyme activity was barely detectable in the conditioned medium or in whole cell extract (Fig. 8B). We then introduced the wild-type or S451A/S452A GGT into bone marrow macrophages through retroviral infection and assessed their osteoclastogenic potential. The results indicate that mutant GGT with essentially no enzyme activity induced osteoclast formation as potently as the wild-type GGT (Fig. 8C). Thus, these results can be taken as evidence that GGT can induce osteoclast development independently of its enzyme activity and raise the possibility that GGT acts as a cytokine on hematopoietic cells in the bone marrow. When the wild-type or pmtGGT was introduced into primary osteoblasts by retroviral infection, both molecules reduced alkaline phosphatase activity (Fig. 8D), suggesting that GGT can act directly on osteoblasts to suppress their differentiation.

Discussion

GGT is recognized as a marker of alcohol consumption and liver disease, and increased serum GGT enzyme activity is a biochemical hallmark of patients with alcoholism, fatty liver disease, and biliary tract disorders such as primary biliary cirrhosis (25). Although it is known that these clinical conditions are risk factors for or complicated by skeletal abnormalities (26–28), the underlying molecular mechanisms are not fully understood. It is demonstrated in the present study that an excess of GGT causes osteopenia and microstructural deterioration characteristic of osteoporosis through an acceleration of osteoclast generation and bone resorption. The serum GGT concentrations in the transgenic model in this study are in the range of 200 IU/liter, a level often seen in individuals with moderately excessive alcohol consumption and in patients with liver and biliary tract diseases. Together with our *in vitro* data showing that purified GGT protein at 100 IU/liter is capable of inducing osteoclast formation in bone marrow cultures (9), it is likely that even moderately elevated circulating levels of GGT would contribute to the bone loss associated with these conditions.

Whereas serum GGT activity derives mainly from the liver, GGT is abundantly expressed in the kidney, pancreas, seminal vesicle, and small intestine, where this ectoenzyme is located on the apical membrane (11). GGT is anchored to the plasma membrane with most of the molecule exposed to extracellular space (11) and is thought to be released by shedding into the serum as well as urine (29), although the exact molecular form in the extracellular fluid as well as the mechanism of shedding remains to be determined. GGT catalyzes the transfer of a γ-glutamyl moiety to an acceptor and plays a critical role in glutathione degradation and cysteine metabolism (10, 11). Mice deficient in GGT exhibit accelerated aging, such as gray fur, cataracts, sexual dysfunction, and severe osteoporosis, and die at the early age of 10–18 wk due to the lack of GGT enzyme activity and the resultant cysteine deficiency (12, 13). Osteopenia in GGT-deficient mice is associated with decreased bone formation, which is treatable by supplementation with *N*-acetylcysteine, suggesting that GGT also plays an important physiological role in regulating bone formation through cysteine metabolism (13). Taken together with the current results, both a deficiency and an excess of GGT result in osteoporosis. However, the osteoporosis is exerted through distinct mechanisms;

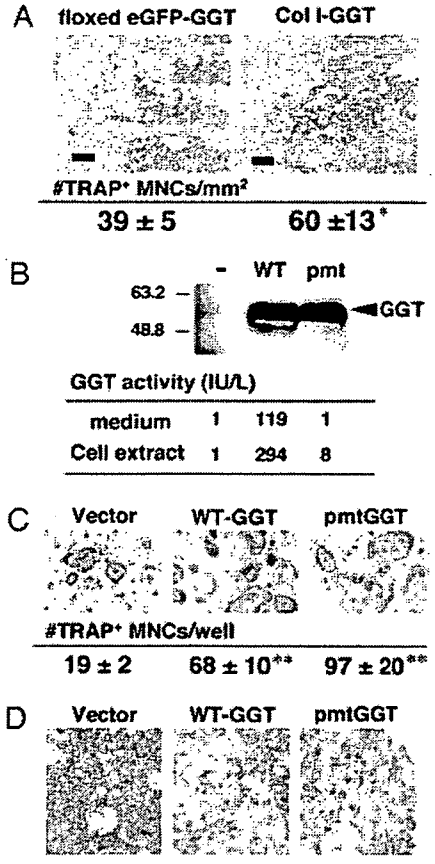

FIG. 8. GGT acts on osteoclast precursors and stimulates osteoclastogenesis independently of its enzyme activity. A, Floxed eGFP-GGT mice were crossed with Col I-Cre mice to generate Col I-GGT mice that expressed GGT specifically in their osteoblasts. The results of staining for TRAP in tibial sections from Col I-GGT mice and floxed eGFP-GGT mice as a control are shown. The number of TRAP-positive multinucleate cells (MNCs) was counted. *, $P < 0.05$ *vs.* wild-type (n = 3 for each group). B and C, pmtGGT with defective enzymatic activity is capable of inducing osteoclast differentiation. S451A/S452A double-mutated GGT (pmtGGT) was introduced into HEK293 cells at the same level as the wild-type (WT) protein, and GGT activity in the conditioned media and cell lysates was determined (B). Bone marrow macrophages were infected with retroviral vectors encoding WT-GGT or pmtGGT and cultured in the presence of M-CSF and RANKL, after which the cells were stained for TRAP activity (C). Note that pmtGGT as well as WT-GGT generated more and larger TRAP-positive osteoclasts. **, $P < 0.01$ *vs.* vector-infected cultures (n = 4 for each group). D, Primary osteoblasts isolated from the calvaria were infected with retroviral vectors encoding WT-GGT or pmtGGT and cultured under osteogenic conditions, after which the cells were stained for alkaline phosphatase activity.

i.e. the former is caused by suppression of bone formation due to systemic deficiency in enzymatic activity, whereas the latter is mainly due to an acceleration of bone resorption by an excess of GGT, which is independent of the enzyme activity and reflects a local effect. The latter nonenzymatic activity of GGT may have been masked by the gene knockout, and appreciating its physiological importance would require the identification of its mediator, possibly the putative receptor.

The results of experiments exploiting targeted overexpression of GGT in osteoblasts driven by a type I collagen promoter suggest not only systemic elevation of GGT but also local production of GGT is sufficient to stimulate osteoclast development. The findings that retroviral transduction of GGT as well as the addition of recombinant GGT protein in bone marrow macrophages stimulates osteoclastogenesis and that bone marrow macrophages from GGT-Tg mice stimulate increased osteoclasts in *ex vivo* cultures further support the concept that hematopoietic cells, especially those of monocyte/macrophage lineage, are the target of GGT in bone. Two cytokines, M-CSF and RANKL, are essential for these progenitor cells to undergo terminal differentiation to become mature, bone-resorbing osteoclasts. Genetic evidence has been obtained by crossing GGT-Tg with RANKL-deficient mice, which shows RANKL is required for GGT action, because GGT is not able to induce osteoclastogenesis in the absence of RANKL. Furthermore, our data show osteoclast progenitor cells from GGT-Tg mice exhibit an enhanced responsiveness to RANKL, resulting in increased generation of osteoclasts at the cellular level and increased expression of critical regulators of osteoclastogenesis, *i.e.* c-Fos, c-Jun, and nuclear factor of activated T cells (NFATc1), at the molecular level. The finding that neither RANKL expression in stromal cells nor RANK expression in bone marrow cells is altered in the presence of an excess of GGT further supports the concept that GGT modulates the signal transduction pathway after RANKL has bound RANK on the surface of osteoclast progenitors. We previously reported the addition of purified GGT protein to marrow stromal cells increased RANKL mRNA and protein at 3 d post addition, which prompted us to hypothesize that GGT stimulates osteoclast formation indirectly through increased RANKL expression (9). The stimulatory effect of GGT on RANKL expression in marrow stromal cells has been confirmed in the current study using recombinant GGT protein but needed a greater concentration (100 ng/ml) than the minimal concentration that exerted the direct effect on bone marrow macrophages (30 ng/ml). Thus, although the exact reason for the difference between these findings and the unaltered RANKL expression in the stromal cells of GGT-Tg mice is not clear, it is likely that hematopoietic cells are more sensitive to the GGT effect than are stromal cells. Also, differences in the molecular form of GGT and/or its duration of action (*i.e.* days in the *in vitro* cultures *vs.* the chronic overexpression for a period of months in the transgenic mice) may be involved. GGT is similar to TGF-β in that both cytokines enhance osteoclast differentiation from hematopoietic cells in response to RANKL (30). However, GGT is dissimilar to TGF-β in that GGT stimulates RANKL expression, whereas TGF-β decreases RANKL and increases OPG expression in stromal cells (31), resulting in complex effects on osteoclastic bone resorption.

Finally and most importantly, the osteoclastogenic function of GGT does not require its enzymatic activity, because the introduction of point mutations in the amino acids critical for enzyme activity had no affect on the osteoclast-inducing activity. These results suggest that a functional domain of GGT required for stimulating osteoclast differentiation is dissociable from its enzymatic activity, and raise the intriguing potential of GGT acting as a local osteoclastogenic cytokine through interaction with a receptor molecule. Alternatively, GGT may modulate the availability of RANKL to RANK through protein-protein interaction. Additional studies are required to identify the putative GGT receptor on osteoclast progenitor cells and to determine whether GGT converges on signaling pathways downstream of the RANK receptor in a cell-autonomous fash-